2024-09-19

Application of Nanosilica with Controlled Particle Size for Performance Enhancement of Cementitious Mixtures

Farjad, Pegah

UNIVERSITY OF CALGARY

Application of Nanosilica with Controlled Particle Size for Performance Enhancement of Cementitious Mixtures

by

Pegah Farjad

A THESIS

SUBMITTED TO THE FACULTY OF GRADUATE STUDIES

IN PARTIAL FULFILLMENT OF THE REQUIREMENTS FOR THE

DEGREE OF MASTER OF SCIENCE

GRADUATE PROGRAM IN CIVIL ENGINEERING

CALGARY, ALBERTA

SEPTEMBER, 2024

ABSTRACT

This study thoroughly investigated the synthesis and application of silica nanoparticles (nanosilica) with controlled sizes to enhance the performance of cementitious mixtures. While nanosilica has been widely studied for its potential to improve cementitious mixture properties, existing studies typically employed commercially available nanosilica with a particular particle size, leaving the effect of particle size variation largely unexplored or resulting in inconsistent or controversial findings regarding its effect on performance. To address this gap, nanosilica were synthesized in-house, enabling precise control over particle size. Techniques such as transmission electron microscopy, dynamic light scattering, ζ-potential, X-ray diffraction, Fourier transform infrared spectroscopy and X-ray photoelectron spectroscopy were employed to characterize the prepared nanosilica samples. The study focused on four distinct particle sizes (10, 35, 65, and 90 nm) to cover the whole range of nanoscale and systematically investigated the compressive strength, hydration, and rheological properties of cement paste incorporating nanosilica at different concentrations of 1, 2 and 3 wt%. Microstructural analyses, including thermogravimetric analysis and quantitative X-ray diffraction, were also conducted on the selected cement pasts incorporating nanosilica to shed light on the mechanisms underlying the performance of nanosilica in the paste. The findings revealed that the smallest particle size of nanosilica (10 nm) provided the highest compressive strength enhancement (over 100% enhancement when used at 2 wt% of cement), surpassing the reported data for the commercially available nanosilica available in the literature. The enhancing effects of the nanosilica particles on the compressive strength of the pastes were less substantial when their particle size increased from 10 to 90 nm. This study provided valuable insights into the effects of nanosilica particle size on the properties of cementitious mixtures, offering a potential pathway for the development of advanced construction materials with superior performance.

ACKNOWLEDGMENTS

First and foremost, I would like to thank my supervisors, Dr. Rahil Khoshnazar and Dr. Nashaat Nassar, for their support and encouragement during my master's thesis. I deeply appreciate their continuous guidance and support.

The synthesis of nanosilica particles was conducted by Dr. Fereshteh Meshkani. I would like to express my deepest gratitude to her for her invaluable support. My sincere thanks also go to Dr. Ahmed Mehairi for his insightful feedback throughout the writing process. I am deeply grateful to my friends and colleagues—Roozbeh, for his assistance with the cement paste testing; Alireza, for his help with the rheological analysis; and Saeed, for his contribution to the microstructural analysis. Your support has been instrumental in the completion of this work.

The financial support provided by the Natural Sciences and Engineering Research Council of Canada (NSERC) and Alberta Innovates is also greatly acknowledged.

Finally, my deepest gratitude goes to my parents and sister for their support, encouragement, and unconditional love, without which I would not have accomplished this important chapter of my life.

To my beloved family

My parents and my sister

Table of Contents

List of Figures

List of Tables

List of Symbols and Abbreviations

ASTM	American Society for Testing and Materials
C-S-H	Calcium-Silicate-Hydrate
C_2S	Dicalcium Silicate
C_3A	Tricalcium Aluminate
C_3S	Tricalcium Silicate
C_4AF	Tetracalcium Aluminoferrite
CH	Calcium Hydroxide
CC	Calcium Carbonate
CVC	Chemical Vapor Condensation
DLS	Dynamic Light Scattering
DTG	Derivative Thermogravimetry
FTIR	Fourier Transform Infrared
GUL	General Use Limestone
LCA	Life Cycle Assessment
PC	Portland Cement
QXRD	Quantitative X-Ray Diffraction
RH	Relative Humidity

SCC	Self-Consolidating Concrete
SEM	Scanning Electron Microscopy
TEM	Transmission Electron Microscopy
TGA	Thermogravimetric Analysis
TEOS	Tetraethyl Orthosilicate
VMA	Viscosity Modifying Admixture
wt%	Weight Percentage
XPS	X-ray Photoelectron Spectroscopy
XRD	X-ray Diffraction
XRF	X-ray Fluorescence
ξ	Zeta potential

1 Chapter 1: Introduction

1.1 Background

Concrete, with an annual production of over 10 billion cubic meters [1] globally, is an inevitable component of modern construction. Production of high-quality concrete, with sufficient strength and durability, is crucial for the sustainability of the construction sector. Concrete properties are influenced by several factors, namely type and content of cementitious materials, water-to-cementitious material ratio (w/cm), and utilization of various admixtures, in addition to mixing and placement methods and curing conditions [2].

In recent years, there has also been an increasing interest in the utilization of nanomaterials in concrete to enhance its performance, such as mechanical strength and durability parameters, or provide it with additional functionalities like self-cleaning properties. Nanosilica has attracted considerable attention [3] among the array of nanomaterials explored in the literature. Researchers have used nanosilica, in the powder or colloidal form, in cementitious mixtures (i.e., cement paste, mortar, and concrete) and reported substantial enhancements in the properties, particularly the compressive strength, of these mixtures [3], [4]. Most of these studies, however, have used commercially available nanosilica with a specific particle size that has been quoted from the manufacturer. Verification of the particle size or more detailed characterization of the nanosilica before utilization in cementitious mixtures is limited in the literature. Furthermore, there are only a few studies that have explored the effect of nanosilica particle size on properties of cementitious mixtures. It is generally perceived that nanosilica with smaller sizes could have a higher ability to enhance the properties of cementitious mixtures. However, there are controversial reports about such effects in the existing literature. Therefore, it is essential to integrate the synthesis and

application of nanosilica with a wide range of particle sizes in one study and provide insight into the effects of nanosilica particle size on the properties of cementitious mixtures.

This study provides a deeper understanding of the nanosilica particle size effects on the performance of cementitious mixtures. It informs concrete materials researchers and practitioners on how to choose a suitable nanosilica particle size for a specific concrete application. Future efforts can focus on both optimizing nanosilica synthesis and mixture design of cementitious mixtures for large-scale application of the nanosilica in the concrete industry.

1.2 Motivation and Novelty Statement

While it is generally accepted in the literature that the utilization of nanosilica can improve the performance of cementitious mixtures, limited studies have explored the effect of varying nanosilica particle sizes on such enhancing effects. Most previous studies have employed commercially available nanosilica with a specific particle size that was reported by the manufacturer without further characterization. In addition, a few studies that include a comparison of the effects of nanosilica with different sizes on the properties of cementitious mixtures have reported inconsistent results. This is likely due to variations in the nanosilica synthesis methods and other nanosilica properties, such as impurities and surface chemistries, as well as their utilization in cementitious mixtures like various dispersion methods and mixing sequences or equipment.

These gaps motivated us to integrate the in-house synthesis and full characterization of nanosilica and its utilization in cement paste in one study. This enabled us to control the nanosilica synthesis parameters to achieve different particle sizes across the nanoscale range. In addition, we fully characterized the in-house prepared nanosilica particles to know our material well before

utilizing it in the cement paste. Lastly, we carried out a detailed characterization and performance assessment of cement paste incorporating the nanosilica particles. With such efforts, not only we achieved a superior strength enhancement with our in-house prepared nanosilica compared to previously reported ones, but also identified a clear trend in the performance enhancement of cement paste incorporating various nanosilica particles with respect to their sizes.

1.3 Objectives

The main objective of this study was to elucidate the effects of nanosilica particle size on the properties of cementitious mixtures, especially compressive strength. To better control the nanosilica particle sizes and investigate their effects, nanosilica particles were prepared in-house and fully characterized with an array of advanced analytical techniques. The nanosilica samples were then added to the cement paste (i.e., mixture of cement and water) in different concentrations. As chemical reactions in cementitious mixtures mainly occur in cement paste, this research focused on studying cement pastes modified by nanosilica additions. Specific objectives of this thesis included the followings:

(1) Synthesize and fully characterize nanosilica of various particle sizes ranging from 10 to 90 nm, and

(2) Apply the controlled size nanosilica particles in cement paste and test the paste for different properties such as compressive strength, heat evolution, microstructure, and rheology.

1.4 Thesis organization

The organization of this thesis is as follows:

- Chapter 1 presents the research background, objectives, and thesis organization.
- Chapter 2 provides an overview of Portland cement and its hydration reactions, given its significance as the primary binding component in cementitious mixtures. This chapter also presents a literature review on nanotechnology and nanomaterials, with a focus on nanosilica. Methods of nanosilica synthesis are discussed, and the chapter concludes with a comprehensive review of the literature on the effect of nanosilica particle size on the performance of cementitious mixtures.
- Chapter 3 introduces the experimental procedure used in this study. The synthesis and characterization of nanosilica with various particle sizes, and the preparation and testing techniques of cement paste samples are described in detail in this chapter.
- Chapter 4 presents the results and discussion of nanosilica characterization alongside the compressive strength, heat of hydration, microstructure, and rheology of cement pastes.
- Chapter 5 summarizes the conclusions and contributions of this thesis to the body of knowledge. It also presents recommendations for future research.

2 Chapter 2: Literature Review

This chapter provides an overview of Portland cement and its hydration reactions, along with an introduction to nanotechnology and nanomaterials. It also includes a literature review on the synthesis methods of nanosilica. The final section offers a comprehensive literature review on the effect of nanosilica particle size on the performance of cementitious mixtures, highlighting gaps in the existing literature.

2.1 Porland cement and its hydration reactions

Portland cement with a worldwide production of around 4.1 billion metric tons annually [5] is the primary binding component in concrete. Partland cement manufacturing starts with the raw materials, primarily clay and limestone, undergoing precise proportioning. In the next step, the raw materials are preheated in a precalciner before being heated to approximately 1,450°C in a rotary kiln. This process yields a product known as "clinker" composed of calcium silicates and calcium aluminates. Clinker is then finely grounded with gypsum to produce Portland cement. The particle size of anhydrous Portland cement typically ranges from 1 to 50 μm [6]. The main phases in Portland cement clinker include tricalcium silicate (C_3S), dicalcium silicate (C_2S), tricalcium aluminate (C_3A), and tetracalcium aluminoferrite (C_3AF). The name of these phases along with their chemical composition, approximate amount in a general use Portland cement clinker, and notation are listed in **Table 2-1**. Among the four major clinker phases, tricalcium silicate is the most important constituent in Portland cement clinker and accounts for approximately 50−70% of the total components. This is followed by dicalcium silicate which constitutes 15−30% of the Portland cement clinker. Tricalcium aluminate and tetracalcium aluminoferrite are relatively minor

phases compared to the two silicate phases, accounting for 5−10% and 5−15% of the Portland cement clinker, respectively [7].

Table 2-1: Main phases in Portland cement clinker [7]

Chemical description	Chemical composition	Name of the phase	Amount	Notation
Tricalcium silicate	$3(CaO).SiO_2$	Alite	50-70 %	C_3S
Dicalcium silicate	$2(CaO).SiO_2$	Belite	15-30 %	C_2S
Tricalcium aluminate	$3(CaO).Al_2O_3$	Aluminate	5-10%	C_3A
Tetracalcium aluminoferrite	$4(CaO).Al_2O_3.Fe_2O_3$	Ferrite	5-15%	C_4AF

Portland cement reacts with water through an exothermic reaction and produces various hydration products. Different phases (i.e., C_3S, C_2S, C_3A, and C_4AF) hydrate at different rates. C_3S reacts relatively quickly during the hydration process and forms calcium-silicate-hydrate (C-S-H) and calcium hydroxide (CH), also known as portlandite. C-S-H is the most important hydration product for developing binding properties in cementitious mixtures. The reaction equation of this hydration process is shown in Eq. 2-1 [8]. C_2S reacts similarly to C_3S, forming C-S-H and CH, but at a much slower rate and producing less CH (Eq. 2-2) [8]. C_3A hydrates in the presence of sulfate to form calcium trisulfoaluminate, also known as ettringite (Eq 2-3) [8]. Over time, this ettringite converts to monosulfoaluminate according to Eq. 2-4 [8]. The abbreviations that are used in these equations are defined in **Table 2-2**.

Table 2-2: Notation in cement chemistry [7].

Composition	Phase	Notation
SiO_2	Silica	S
Al_2O_3	Alumina	A
CaO	Calcium oxide	C
SO_3	Sulfate	$\overline{S}$
H_2O	Water	H

$$C_3S + 5.3\ H \rightarrow C_{1.7}\ SH_4 + 1.3\ CH \qquad \text{Eq. 2-1}$$

$$C_2S + 4.3\ H \rightarrow C_{1.7}\ SH_4 + 0.3\ CH \qquad \text{Eq. 2-2}$$

$$C_3A + 3\ C\overline{S}H_2 + 26\ H \rightarrow C_6A\overline{S}_3H_{32} \qquad \text{Eq. 2-3}$$

$$C_6A\overline{S}H_{32} + 2\ C_3A + 4\ H \rightarrow 3\ C_4A\overline{S}H_{12} \qquad \text{Eq. 2-4}$$

Hydration reactions are an ongoing process and, through time, the hydration reaction products form and shape the microstructure of a hardened cementitious mixture. The hydration rate is initially determined by the dissolution rate of the clinker phases, then by the nucleation and precipitation rate of hydrated ones, and ultimately by the diffusion rate of water and dissolved ions into the layer of hydrated phases [7]. The main part of Portland cement hydration reactions is usually completed by the age of 28 days [6]. The presence of impurities and different minerals and oxides in the composition of Portland cement besides the addition of chemical admixtures and additives would influence the hydration process and make it very complex [9].

Improving the performance of cementitious mixtures for specific applications has always been a priority. To achieve desired properties, various admixtures like water reducers, air-entraining agents, set-accelerators, and set-retarders are commonly employed. In recent years, nanomaterials have garnered significant attention as advanced admixtures for enhancing the

performance of cementitious mixtures, leading to improvements in strength, durability, and overall microstructure of these mixtures [10].

2.2 Nanotechnology and Nanomaterials

Nanotechnology is the science and engineering of investigating, observing, and altering the performance of materials at the nanoscale, which ranges from 1 to 100 nanometers, at least in one dimension [11]. Nanomaterials, formed by the rearrangement and alteration of bulk materials at the nanoscale, have attracted significant attention since the development of nanotechnology. At the nano-level, materials exhibit properties that are a combination of traditional physics and quantum mechanics. At this scale, the physical, chemical, and biological characteristics of materials fundamentally differ from those of individual atoms or bulk matters. Consequently, materials at the nanoscale can display novel properties that are not observable at larger scales.

There are two main approaches for the synthesis of nanomaterials: top-down and bottom-up approaches (**Figure 2-1**). In the top-down approach, nanomaterials are synthesized by dividing the materials into smaller units until the nanoscale is achieved [11]. This approach includes processes like mechanical milling [12] or electron beam lithography [13]. Top-down approaches have certain limitations. The resolution and replication speed limited the efficacy, when the sizes go below 100 nm [14]. In the bottom-up approach, nanomaterials are made at the atomic scale, then scaled up to be used in large-scale production. The sol-gel method is a promising way of nanomaterials production in the bottom-up approach [14] which is further described in Section 2.2.2.

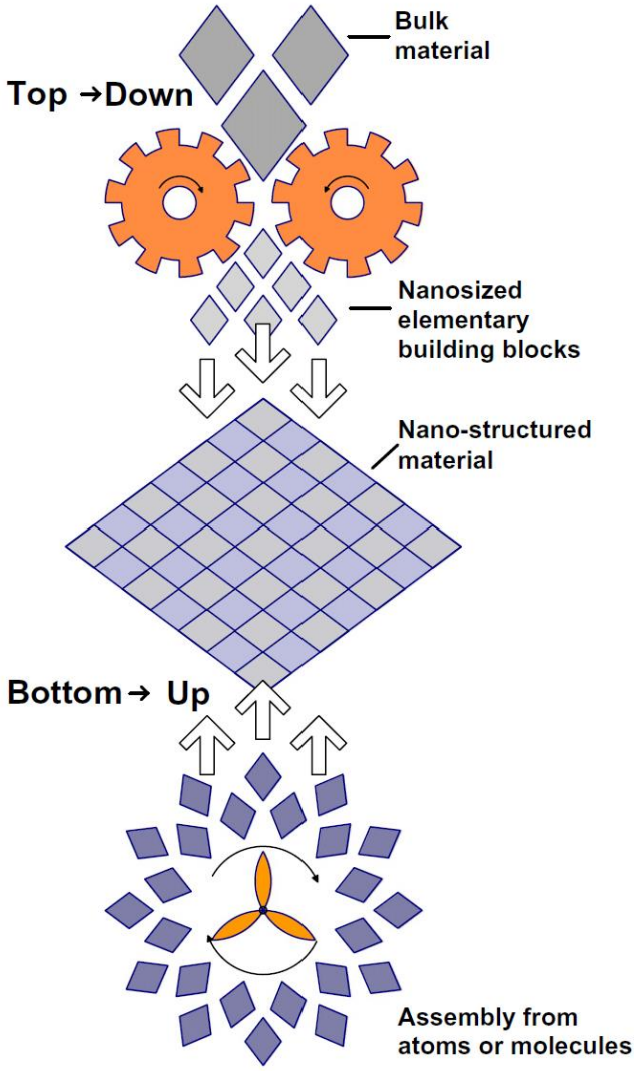

Figure 2-1: Schematic representation of the top-down and bottom-up approaches used for the synthesis of nanomaterials. Adapted with permission from Sanchez and Sobolev [11], Copyright 2010 Elsevier.

2.2.1 Application of Nanomaterials in Cementitious Mixtures

Various nanomaterials have been used as additives in cementitious mixtures to provide enhanced performance (such as strength and durability) or additional functionalities (such as self-cleaning and self-sensing) [15]. These nanomaterials are typically classified based on their dimensions, chemical composition, and reactivity in cementitious mixtures [16], [17], [18], [19]. Zero-

dimensional nanomaterials are classified as nanomaterials with all the dimensions below 100 nm. Nanoparticles of SiO_2 [3], [20], Fe_3O_4 [21], $CaCO_3$ [22], [23], Al_2O_3 [24], and TiO_2 [25] are among the most popular zero-dimensional nanomaterials with applications in cementitious mixtures. One-dimensional nanomaterials have two dimensions below 100 nm. Examples include carbon nanotubes [19] and carbon nanofibers [26], both of which are used in cementitious mixtures. Two-dimensional nanomaterials have one dimension below 100 nm. Graphene oxide is an example of this group of nanomaterials that has been used in cementitious mixtures [27].

In another classification based on the chemical composition of nanomaterials, they can be organic, inorganic, or carbon-based [28]. Furthermore, nanomaterials may be either non-reactive or reactive, when utilized in cementitious mixtures. Non-reactive nanomaterials may act as nucleation sites, fillers, and/or bridges between hydration products, whereas reactive ones participate in chemical reactions in cementitious mixtures [19]. These classifications are shown in **Figure 2-2.** Nanosilica, which is classified as an inorganic nanoparticle (zero-dimensional nanomaterial) with reactive properties in cementitious mixtures, has attracted considerable attention among the array of nanomaterials explored in the literature. Therefore, different methods of nanosilica synthesis and their application in cementitious mixtures are discussed in the following section.

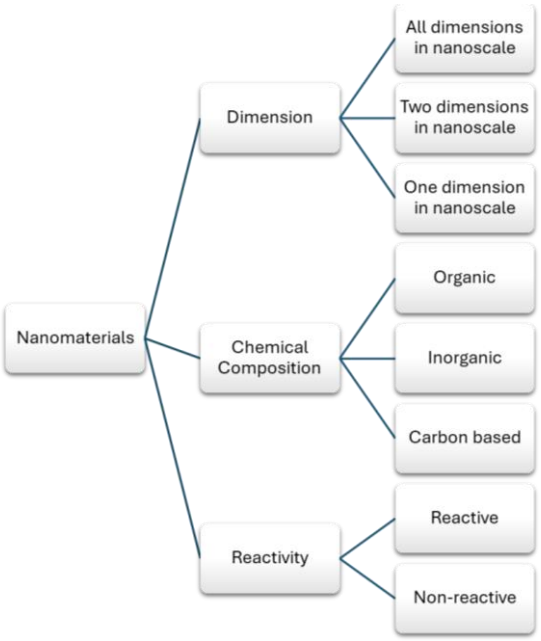

Figure 2-2: Schematic representation of nanomaterials classification.

2.2.2 Nanosilica Synthesis Methods

Several methods have been used to synthesize nanosilica [29]. Sol-gel method is the most commonly used method for producing nanosilica particles [30]. Other methods such as reverse microemulsion [31] and flame synthesis [32], [33] have also been used for nanosilica synthesis. In the reverse microemulsion method, surfactant molecules in organic solvents form spherical reverse micelles, which create microcavities in the presence of water. These microcavities, known as reverse micelles, serve as nucleation sites for nanoparticle growth when silicon alkoxides and a catalyst are added. This method is expensive and involves challenges in removing surfactants from the final product [31]. Another method for producing nanosilica particles is high-temperature flame synthesis, also known as chemical vapor condensation (CVC). In the CVC method, nanosilica particles are formed by reacting silicon tetrachloride ($SiCl_4$) with hydrogen and oxygen

[32]. Despite its widespread use for commercial production of nanosilica particles in powder form, this method poses difficulties in controlling particle size, morphology, and phase composition [34].

The sol-gel method is another synthesis method that has been used to produce silica, nanosilica, glass, and ceramic materials due to its ability to create pure and homogeneous products under mild conditions. This process involves hydrolysis and condensation of metal alkoxides, such as tetraethyl orthosilicate (TEOS), or inorganic salts such as sodium silicate (Na_2SiO_3), in the presence of a catalyst, typically an inorganic acid (e.g., HCl) or a base (e.g., NH_3) [35]. The hydrolysis of TEOS produces silanol groups, which then undergo condensation or polymerization to form siloxane bridges (Si–O–Si), building the nanosilica structure. The formation of nanosilica particles occurs in two stages: nucleation and growth. The sol-gel method is widely used because it allows for controlling the synthesis parameters and yielding high-quality nanosilica particles. A pioneering study based on sol-gel method by Stöber et al. [36] successfully synthesized spherical and monodispersed silica and nanosilica particles ranging from 5 to 2000 nm using aqueous alcohol solutions of silica alkoxides with ammonia as a catalyst under basic conditions (pH >7). The Stöber method is notable for its potential to produce monodispersed spherical nanosilica particles.

2.2.3 Nanosilica Particle Size Effect on the Performance of Cementitious Mixtures

Nanosilica has been incorporated by many researchers into cementitious mixtures either as a powder or in colloidal form [37]. In these studies, they commonly used nanosilica particles with sizes ranging from 5 to 40 nm [3], [4], [20], [38], [39], [40], [41], [42], [43], [44], [45]. Nanosilica offers the potential to enhance the performance of cementitious mixture through three primary

mechanisms, namely: filling effect, nucleation effect, and pozzolanic reaction [46], [47], [48]. The filling effect refers to filling the pores inside the cementitious matrix with nanosilica particles resulting in a denser matrix [49]. Furthermore, nanosilica accelerates the Portland cement hydration process by providing extra nucleation sites for the formation of the hydration products. Finally, its pozzolanic reaction with CH, formed due to the hydration of Portland cement, generates additional C-S-H within the hydrated matrix [51]. Although significant improvements of mechanical and durability properties of cementitious mixtures have been reported due to the addition of nanosilica, most of the previous studies have utilized nanosilica of a specific size that was commercially available and not tailored for performance improvement of cementitious mixtures [39], [52].

Particle size is one of the important characteristics of nanosilica and can significantly affect its performance in cementitious mixtures. However, the number of existing research on the effect of different particle sizes of nanosilica on the performance of cementitious mixtures is limited. **Table 2-3** presents literature that investigated the utilization of nanosilica with different particle sizes on the performance of cementitious mixtures. Most of these studies have focused on nanosilica with relatively small particle sizes, with only a few of them exceeding 50 nm. Moreover, they did not cover the whole nano range in one study, and they did not necessarily get better performance when using smaller sizes. For example, Bolhassani and Samani [53] studied the effect of three different nanosilica particle sizes (7, 12, and 20 nm) in powdery form and two sizes (12 and 25 nm) in colloidal form, as well as silica fume, on the performance of cement paste and mortar mixtures. They reported that all the nanosilica additions enhanced the compressive strength of the pastes at the age of 7 and 28 days, with the highest increase (80% and 54% at the two tested ages) observed for the paste incorporating 3 wt% nanosilica with a 20 nm particle size (specific surface

area of 90 m^2/g) although it was the largest size among the powdery forms that were tested. The nanosilica additions did not provide similar levels of strength enhancement in mortar samples compared to the pastes. The addition of 7 wt% nanosilica with a 20 nm particle size in mortars only provided an increase of ~13% in their compressive strength. Haruehansapong et al. [54] also investigated the effect of nanosilica powders with particle sizes of 12, 20 and 40 nm on the compressive strength of mortar samples. They emphasized the favorable effect of larger nanosilica particles (40 nm compared to 20 and 12 nm) on the compressive strength gain of mortars with approximately 55% enhancement compared to reference mortar at 28 days curing age.

Khaloo et al. [55] studied the effect of colloidal nanosilica with particle sizes of 7 and 12 nm in high-performance concrete with water-to-binder ratios (w/b) of 0.25, 0.30, and 0.35. Their findings revealed that the highest improvement in compressive strength occurred with the incorporation of 1.5 wt% of 12 nm nanosilica into the mixture with a water-to-binder ratio of 0.35. In another study, nanosilica with 15 nm particle size led to the highest enhancement in the 7-day compressive strength of concrete (w/b of 0.6) when it was compared to nanosilica with 5 and 98 nm particle sizes [37]. Maggi and Jun [56] utilized the same nanosilica particle sizes as Haruehansapong et al. [54] for oil-well cement slurry in their research and observed higher early compressive strength and increased pozzolanic reactivity with 40 nm nanosilica compared to 12 and 20 nm. All these studies utilized commercial nanosilica, and there are only a few studies that explored the effect of in-house prepared nanosilica with varying particle sizes in cementitious mixtures. Zhang et al. [50] investigated the effect of in-house synthesized colloidal nanosilica with particle sizes of 30, 60, and 140 nm (the last one being outside the nano-scale range) in cement paste. Nanosilica with 60 nm particle size was reported to be the most effective one, albeit with only ~ 11% compressive strength enhancement at 28 days. Additionally, other studies investigated

the effect of different nanosilica sizes on their pozzolanic reactivity (9, 15, and 30 nm) [47], cement hydration kinetics (15 and 50 nm) [57] and water permeability (12, 20, and 40 nm) [58] without any investigation on the strength gain of these mixtures. It is important to note that most previous studies did not include any characterization of nanosilica, making it difficult to verify the data provided by manufacturers.

Table 2-3 shows no general agreement on whether there is a trend in the performance enhancement of cementitious mixtures with varying nanosilica particle sizes, as results vary across studies. This variation could be attributed to several factors, including the use of commercially available nanosilica, where differences in synthesis methods may affect the particle size, specific surface area, purity and chemical composition, morphology, surface properties and reactivity of the nanosilica particles and, consequently, their performance in the cementitious mixtures [49], [59]. Additionally, most studies used nanosilica in powder form and used different dispersion methods in cementitious mixtures that can affect the effects of nanosilica on the properties of these mixtures. Some studies simply added the nanosilica powders to the water and mixed them for a specific time [53], [57], [58], [54], [46], while others used a sonication bath [48] or ultrasonication device [60], [61] to disperse the particles in water or incorporated dispersant materials into their mixtures [56]. There were also reports that did not specify the dispersion method used for the powder nanosilica particles [62]. It is also important to note that properties of the cementitious mixtures varied across different studies (i.e., type of cementitious mixture, w/b, type and concentration of additives), which can also influence the effectiveness of nanosilica particles of different sizes. These variations in mixture properties may contribute to the inconsistent results observed in the performance enhancement of cementitious mixtures incorporating nanosilica with different particle sizes reported in the literature.

In summary, while researchers have made considerable efforts to explore the effect of varying particle sizes of nanosilica on the performance of cementitious mixtures, their findings were controversial. In addition, there were research gaps such as (i) a lack of comprehensive coverage across the wide range of nanoscale, (ii) limited utilization of characterization analysis for different nanosilica particle sizes, and (iii) scarce investigation into the in-house preparation of nanosilica with control over their sizes and their utilization in cementitious mixtures for performance enhancement. This study aimed to address these gaps through an experimental program that is discussed in the following chapter.

Table 2-3: Characteristics of nanosilica with different particle sizes and their effects on the performance of cementitious mixtures.

Nanosilica characteristics				**Nanosilica application in cementitious mixtures**				**Reference**
Particle size (nm)	**SSA (m^2/g)**	**Form**	**Concentration (wt%)**	**Type of cementitious mixtures**	**Water/ binder**	**Parameters studied**	**Main findings**	
7-40	422	Powder	0.5, 1, 1.5	Paste	0.5	Rheology, Heat of hydration	The paste containing 40 nm nanosilica exhibited the highest viscosity, yield stress, and heat flow peak.	[61]*
100	249							
200**	206							
20-50	100	Powder	0.6, 0.9, 1.2	Paste	0.5	Compressive strength, Heat of hydration, Porosity	The paste containing nanosilica with SSA of 470 m^2/g (20 nm) exhibited higher strength, greater heat flow peak, and lower porosity at the optimum concentration of 0.9 wt%.	[48]*
	470							
12	220	Powder	1, 2,3,4	Oil well cement paste	0.45	Early compressive strength, Microstructure	The paste containing 40-nm nanosilica exhibited the highest early strength enhancement (40% at 36 h and 3 wt%) and pozzolanic reactivity.	[56]*
20	90							
40	50							

Nanosilica characteristics				Nanosilica application in cementitious mixtures				Reference
Particle size (nm)	**SSA (m^2/g)**	**Form**	**Concentration (wt%)**	**Type of cementitious mixtures**	**Water/ binder**	**Parameters studied**	**Main findings**	
15	250	Powder	2	Paste	0.37	Compressive strength, Microstructure	The paste containing 50-nm nanosilica exhibited higher strength, while samples with 15-nm nanosilica demonstrated a denser microstructure as detected by mercury intrusion porosimeter (MIP) test.	[62]*
50	200							
36	-	Colloidal	0.5, 1, 1.5, 2, 3, 4	Paste	0.3-0.6	Rheology, Compressive strength	The paste containing 264-nm nanosilica exhibited higher strength, and better flow based on rheology test.	[63]
264**								
30	-	Colloidal	5	Paste	0.5	Compressive strength, Flowability, Microstructure	The paste containing 60-nm nanosilica exhibited the highest strength improvement (11% at 28-days), flowability and denser structure based on SEM.	[50]*
60								
140**								

Nanosilica characteristics				Nanosilica application in cementitious mixtures				Reference
Particle size (nm)	**SSA (m^2/g)**	**Form**	**Concentration (wt%)**	**Type of cementitious mixtures**	**Water/ binder**	**Parameters studied**	**Main findings**	
9	300	Colloidal	1, 2, 3, 5, 7.5	Paste	0.27	Pozzolanic reactivity, Hydration degree, Setting time	The paste containing 9-nm nanosilica exhibited faster pozzolanic reactivity especially at early age (start from 9h) and higher initial setting time. Hydration degree of pastes with 30-nm nanosilica was slightly higher compared to others at 1 day, while at later ages (100 days) they were comparable.	[47]
15	200							
30	100							
15	200	Powder	0.5, 1, 3	Paste	0.4	Compressive strength, Flowability	The paste containing 15-nm nanosilica exhibited the highest strength improvement of 70% at 28-days and 3 wt%. It also decreased the paste flow.	[60]
30	100							
1-3	500	Colloidal	3, 5, 10	Mortar	0.4	Compressive strength, Water absorption, Microstructure	Mortars containing 1-3 nm nanosilica at 3 wt% and 35-75 nm at 5 wt% and 10 wt %, showed higher strength and lower water absorption and denser microstructure.	[64]*
8-15	250							
35-75	80							

Nanosilica characteristics				Nanosilica application in cementitious mixtures				Reference
Particle size (nm)	**SSA (m^2/g)**	**Form**	**Concentration (wt%)**	**Type of cementitious mixtures**	**Water/ binder**	**Parameters studied**	**Main findings**	
15	250	Powder	2	Mortar	0.37	Hydration kinetic modeling	Mortars containing 15-nm nanosilica accelerated hydration rate in early ages (before 1 day) more effectively.	[57]*
50	200							
12	-	Powder	9	Mortar	0.65	Water permeability, Abrasion resistance, Shrinkage	Mortars containing 40-nm nanosilica exhibited the highest resistance to abrasion and lowest water permeability. Samples with NS of 12 and 40 nm exhibited higher drying shrinkage in comparison to reference and samples with 40 nm nanosilica.	[58]*
20								
40								
7	380	Powder	0.5, 1.5, 3, 5, 7	Mortar, Paste	0.48	Compressive strength, Microstructure	The paste containing 20-nm nanosilica exhibited the highest strength improvement (80% and 54% at 7 and 28 days) with 3 wt% concentration. The effect on mortars was not as significant as pastes. Adding a high concentration of 20-nm nanosilica (7 wt%) provided the same effect as using micro silica (7 wt%) in mortars with strength enhancement of 12% at 28 days.	[53]*
12	200							
20	90							
12	150	Colloidal						
25	80							

Nanosilica characteristics				Nanosilica application in cementitious mixtures				Reference
Particle size (nm)	**SSA (m^2/g)**	**Form**	**Concentration (wt%)**	**Type of cementitious mixtures**	**Water/ binder**	**Parameters studied**	**Main findings**	
12	-	Powder	3, 6, 9, 12	Mortar	0.65	Compressive strength, Microstructure	Mortars containing 40-nm nanosilica exhibited the highest compressive strength improvement at 9 wt% concentration. All the nanosilica incorporated samples showed a denser microstructure based on SEM images.	[54]*
20								
40								
5	500	Colloidal	0.25, 0.5, 0.75, 1, 1.25, 1.5, 2, 3	Concrete	0.4, 0.5, 0.6	Compressive strength, Water absorption, Microstructure	Concretes containing 15-nm nanosilica exhibited the highest strength followed by 5-nm and 98-nm. The optimum concentration of nanosilica in the mixtures become higher as the size of them increased, however it was found to be in the range of 2 to 5 wt% based on the w/b ratio and particle size. Water absorption considerably decreased when nanosilica particles were used in concrete, especially with higher w/b ratios and the pore structure was improved.	[37]*
15	250							
98	52							
7	380	Colloidal	0.75, 1.5	High performance concrete	0.25, 0.3, 0.35	Compressive strength, Flowability Microstructure	Concretes containing 12-nm nanosilica had higher compressive strength. By decreasing the water to binder ratio, 12-nm nanosilica performed better than 7-nm nanosilica in enhancing the compressive strength performance. 7-nm nanosilica particles had a higher pozzolanic reactivity and more reduction of flow based on slump test.	[55]*
12	200							

Nanosilica characteristics				Nanosilica application in cementitious mixtures				Reference
Particle size (nm)	**SSA (m^2/g)**	**Form**	**Concentration (wt%)**	**Type of cementitious mixtures**	**Water/ binder**	**Parameters studied**	**Main findings**	
15	160	Powder	0.5, 1, 1.5, 2	Concrete	0.4	Compressive strength, Tensile strength	Concretes containing 80-nm nanosilica at 28 days exhibited 19% compressive strength enhancement with 2 wt%. This amount was around 8% for samples with 15-nm nanosilica. The highest tensile strength was achieved with 80-nm nanosilica at the age of 91 days with 100% enhancement compared to reference concrete.	[46]*
80	560							

* The nanosilica particle sizes mentioned in these references are cited without verified characteristics of their sizes, as they are primarily sourced from manufacturers.
** These sizes cannot be classified in the nanoscale range (i.e., they are larger than 100 nm).
SSA= Specific surface area

3 Chapter 3: Experimental Program

3.1 Materials

Materials used for the synthesis of nanosilica particles included tetraethyl orthosilicate (TEOS, 99 wt% purity) from Merck (Italy) as a precursor, and ammonium hydroxide (NH_4OH, 28-30 wt% purity) and ethanol (EtOH, 90 wt% purity) from Sigma-Aldrich (Canada). Distilled water was also used in the nanosilica synthesis process.

General use Portland limestone cement (GUL), Lafarge, Canada, complying with the Canadian Standard Association (CSA) A3001 was used to prepare the cement pastes upon mixing with distilled water. The main oxide composition of the Portland cement, as obtained by the X-ray fluorescence (XRF), and its loss on ignition are also presented in **Table 3-1**. Isopropyl alcohol (IPA, 99.5 wt% purity) (Fisher Scientific, Canada) was also used in this study to stop the chemical reactions in cement pastes at specific ages.

Table 3-1: Main oxide composition and loss on ignition of the general use Portland limestone cement.

Component	**SiO_2**	**Al_2O_3**	**Fe_2O_3**	**CaO**	**MgO**	**SO_3**	**Loss on Ignition**
wt%	18.30	3.93	3.34	60.81	4.16	3.43	5.02

3.2 Methods

3.2.1 Nanosilica Synthesis

Five different batches of nanosilica with different particle sizes were prepared using the Stöber method [36]. This method utilized the hydrolysis and condensation of tetraethyl orthosilicate (TEOS) in an ethanol solution, with ammonia acting as a catalyst. By adjusting the concentration of the reagents and the reaction conditions, the size and uniformity of the particles could be precisely controlled [36], [65].

The steps used for nanosilica synthesis in this study are shown schematically in **Figure 3-1**. The synthesis parameters, including the quantities of ethanol, ammonia, water, and TEOS, were specified. In the first step, ethanol with volumes of 20, 25, 40, 60, and 100 mL was mixed with 80 mL of distilled water for 10 min at room temperature using a magnetic stirrer. Then, 15 mL of ammonia was added to this solution and mixing continued for 10 min. This was followed by adding 12.5 mL of TEOS. Magnetic stirring was continued for 20 h at ambient temperature. Finally, the precipitated particles in the solution were centrifuged and washed 5 times with distilled water. In total, 200 mL of distilled water was used for washing each 1 g of nanosilica particles. The nanosilica particles were recovered as colloidal suspensions for using in the cement paste (**Figure 3-2**). Particle size was controlled by adjusting the amount of ethanol in each synthesis. Ethanol is one product of the hydrolysis of TEOS. Since hydrolysis of TEOS is a reversible reaction, using ethanol as a solvent would raise the rate of backward reaction. Consequently, this resulted in a low net hydrolysis rate and larger particles [66], [67]. The effect of pH (with the amount of ammonia) and aging time on the particle size of the nanosilica particles was also studied and the results are provided in Appendix A.

In each batch, DLS and ζ-potential analysis were conducted at 25 ^{o}C using a Zetasizer (Malverin Instruments Limited, UK) to evaluate the hydrodynamic diameter (D_h) of the nanosilica particles and their stability in aqueous solutions. 0.5 mL of each nanosilica sample was diluted with 20 mL of distilled water and poured into the disposable cell for each measurement. The results are reported in **Table 3-2**.

Figure 3-1: Synthesis steps of nanosilica particles. Step1: mixing water and ethanol, Step 2: adding ammonia, Step 3: adding TEOS, Step 4: continuous mixing for 20 h, Step 5: centrifuging.

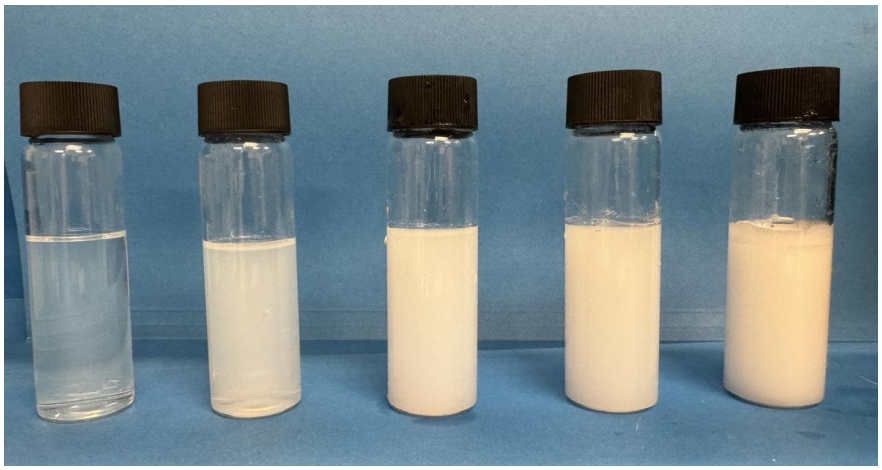

Figure 3-2: Photograph of synthesized nanosilica particles in colloidal form with different particle sizes. From left to right: N1 to N5, as described in Table 3-2.

Table 3-2: Synthesis parameters, hydrodynamic diameter (D_h), and ζ-Potential of nanosilica samples.

Sample ID	Synthesis parameters					Characteristics	
	TEOS (mL)	Water (mL)	Ammonia (mL)	Ethanol (mL)	Aging (h)	D_h (nm)	ζ-Potential (mV)
N1	12.5	80	15	20	20	13	-42
N2				25		38	-41
N3				40		70	-40
N4				60		91	-48
N5				100		108	-43

The first four samples (N1 to N4) were selected for further investigation on cement paste performance (**Table 3-2**). These selected samples were fully characterized, and the results were discussed in Section 4.1. This selection and analysis addressed the research gaps identified in the previous chapters of the thesis (addressing the entire nanoscale range).

3.2.2 Cement Paste Preparation

Cement pastes were prepared with a constant water-to-cement ratio (w/c) of 0.42. A total of 12 cement paste mixtures including the reference paste and pastes incorporating various sizes of nanosilica (10, 35, 65, and 90 nm) at three weight percentages (1, 2, and 3 wt%) were prepared. For each nanosilica sample, the water content in the nanosilica solution was calculated. This amount was then subtracted from the total water required based on the w/c in cement pastes. The calculated water was added to the nanosilica solution to ensure the correct water content. Then, 100 g of Portland cement was added to the mixture of 42 mL water and nanosilica. After 30 s rest, the mixture was shear mixed using an Ultra-Compact Digital Mixer (Cole-Parmer OS-200 series, Canada) for 30 s at a medium speed of 900 rpm and then for 1 min at a high speed of 1200 rpm, similar to the steps described in ASTM C305 [68]. This process is shown in **Figure 3-3**. Following the preparation of the cement pastes, they were cast in 10 × 10 ×10 mm^3 molds and tapped against the flat surface three times to ensure sufficient compaction (**Figure 3-4**). All molds were covered with polyethylene sheets to prevent evaporation from their surface. After 24 h, the samples were de-molded (**Figure 3-5**) and kept in a curing room at a temperature of 23 °C and relative humidity (RH) of 98% until the desired testing age.

To represent cement pastes with varying concentrations of nanosilica of different particle sizes, the pastes were labeled as NS followed by two numbers that showed the mean particle size of the nanosilica used in that paste and concentration of the nanosilica based on the cement weight, respectively. For example, NS10-1 indicates a cement paste containing nanosilica with 10 nm particle size at a concentration of 1 wt%. Additionally, "ref" refers to the cement pastes without nanosilica (i.e., control sample).

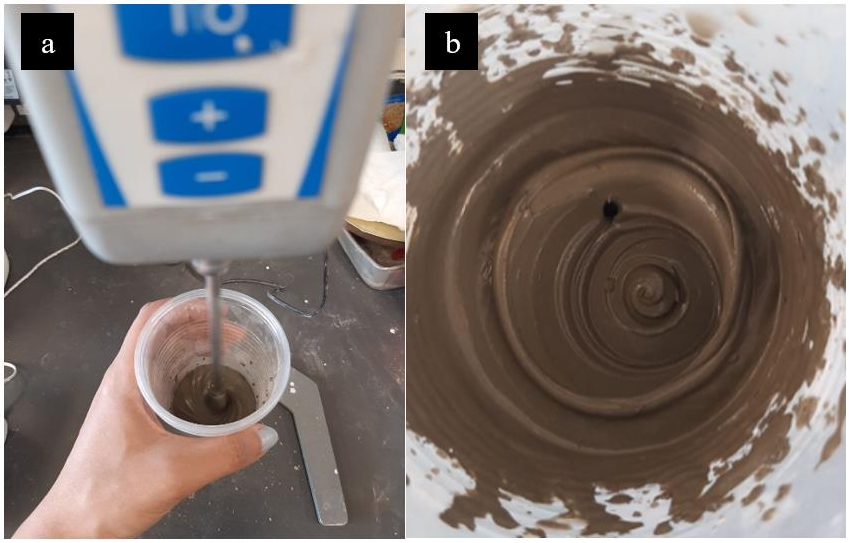

Figure 3-3: Photographs of a) Mixing of cement paste using the Ultra-Compact Digital Mixer, b) Cement paste after mixing.

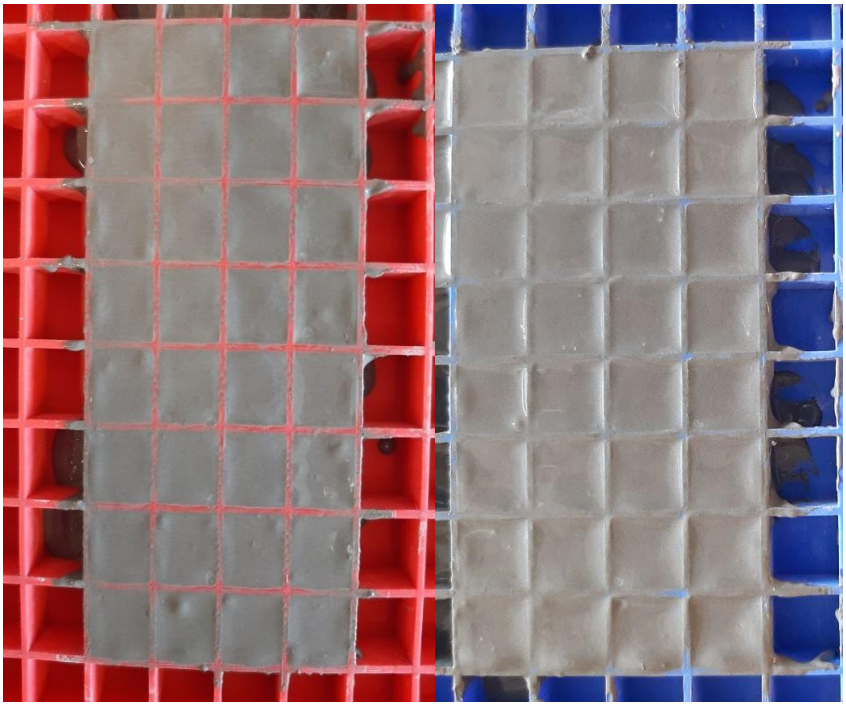

Figure 3-4: Photographs of cement paste in 10×10×10 mm^3 molds.

Figure 3-5: Photograph of hardened cement pastes for the compressive strength test.

3.2.3 Characterization and Testing Techniques

The characterization and testing of samples were divided into two main categories. First, nanosilica particles were fully characterized. Then, their effect on the performance of cement pastes was studied by testing the cement pastes incorporating nanosilica of various sizes. Characterization and testing techniques are described in detail in this section.

3.2.3.1 Characterization of Nanosilica

All nanosilica samples were characterized using transmission electron microscopy (TEM), dynamic light scattering (DLS), ζ-potential, X-ray diffraction (XRD), Fourier transform infrared spectroscopy (FTIR), and X-ray photoelectron spectroscopy (XPS). TEM was used to study the shape and particle size of nanosilica samples with a Tecnai F20 200 kV TEM (FEI, USA). About 1 mL of each nanosilica sample in its colloidal form was used for the TEM. The particle size of nanosilica was obtained by using Image J software and analyzing the TEM images. The diameter of minimum 80 particles was considered for the robustness of the data in image analysis. The

particle size distribution of each nanosilica was plotted, and the average particle size was calculated.

XRD, FTIR, and XPS tests were performed on powdered nanosilica samples which was obtained by drying the colloidal nanosilica in a vacuum oven at 60 ˚C for 24 h and then grinding in a mortar and pestle. The analysis was conducted at room temperature (~ 23˚C). The XRD analysis was conducted using a Bruker D8 Advance ECO diffractometer (USA) equipped with a Cu Kα X-ray source (λ = 0.154178 nm) operating at 40 kV and 25mA. The data were collected in a 2θ range of 5 – 70^{o} with a step size of 0.0132^{o} and a step time of 0.56 s per step range.

FTIR spectra of the nanosilica powders were recorded on a spectrophotometer (Shimadzu IRAffinity-1S FTIR, Mandel, Japan) at room temperature and in regular mode. About 1 mg of each nanosilica powder was blended with 100 mg of KBr as a reference. The measurements were taken at wavenumbers ranging from 4000 to 400 cm^{-1}, with a resolution of 4 cm^{-1} and a total of 50 scans per sample.

The nanosilica powders were also tested by the XPS for surface chemistry analysis. XPS was performed with an Escalab QXi spectrometer (Thermo Scientific, USA) employing a monochromatic Al Kα X-ray source (1486.6 eV) with a 650 µm × 200 µm spot size. The operating vacuum condition of the analysis chamber was 8 mbar. About 0.1 mg of nanosilica samples were mounted on a double-sided carbon tape attached to the sample holder. Survey scans were collected using a pass energy of 150 eV at 1.0 eV/step.

3.2.3.2 Testing of Cement Pastes

The compressive strength of cement pastes was measured using a compressive strength test machine (RIEHLE, USA), shown in **Figure 3-6**, at the ages of 7, 28 and 91 days. Seven cement pastes were tested at each age to ensure the robustness of the measurements, and the average and standard deviation of the results were reported.

Figure 3-6: Photograph of the compressive strength equipment used in this study.

A TAM Air isothermal calorimeter (TA Instruments, USA) was used to measure the heat evolution of the cement pastes for 7 days at 23 ± 0.02 °C according to ASTM C1702 [69] (**Figure 3-7**). The baseline for the experiment was established 24 h before starting the main test by placing quartz sand with the same thermal mass as the tested samples in reference cells of the calorimeter. For each sample, approximately 20 g of cement paste was prepared in a plastic container. Then,

about 10 g of the paste was poured into glass vials and placed in testing cells of the calorimeter and the data were recorded with TAM Air Assistant software.

Figure 3-7: Photograph of the isothermal calorimeter used in this study.

TGA and QXRD were performed on powdered cement pastes at the ages of 1, 7 and 28 days to study their microstructure. Hardened cement pastes were submerged in isopropanol for 7 days to stop the chemical reactions. After removing the samples from the isopropanol, they were stored in a desiccator for 1 day. They were then ground into powder using an agate mortar and pestle.

TGA was conducted using an SDT650 (TA Instruments, USA). This instrument is shown in **Figure 3-8**. About 30 mg of each powdered cement paste was placed in the TGA pan. The analysis was carried out under a constant nitrogen flow of 25 mL/min. To ensure a reference starting status for all the samples, the procedure began with heating the samples at 40°C for 45 min. The samples were subsequently subjected to heating from 40 °C to 1000 °C with a ramp of

10 °C/min. The amount of calcium hydroxide (CH) was calculated by integrating its characteristic peak over the range of 400 – 500 °C in the differential thermogravimetric curve (DTG). The calculated mass loss of CH was then normalized to the weight of cement at 600°C, following the methodology outlined by Scrivener et al. [70]. The peak between 600 °C and 800 °C was attributed to the decomposition of calcium carbonates (CC). The CC content of the plain cement was around 10%; therefore, the CH content in each cement paste was calculated to find the corrected CH content while considering the carbonation effect, although this amount was small [70].

Figure 3-8: Photograph of the thermogravimetric analyzer used in this study.

QXRD was performed on cement pastes to identify their crystalline phase assemblage and amorphous content at desired ages. To perform the test, powdered cement pastes were weighed and mixed with 20 wt% corundum [70]. Then, the XRD test was performed on them the same as the procedure that was described for the XRD test on nanosilica particles. Rietveld method [70]

was performed using Profex-BGMN software [71] for quantification of different phases in cement pastes.

Rheology measurements were carried out in a Modular Compact Rheometer, MCR302 (Anton Paar, Switzerland), equipped with a bob and cup measurement system with serrated bob geometry (**Figure 3-9**). The diameters of the bob and cup were 26.660 and 28.906 mm, respectively, providing a shear gap of 1.123 mm. The fresh cement pastes were poured into the cup 15 min after the first contact between water and cement. This time was considered to allow the hydration process to enter the dormant period [72], as the cement phase dissolves very quickly upon first contact with water, making the mixture unstable for measuring rheological behavior before this period. A flow test was conducted to measure the changes of shear stress against shear rate using the protocol shown in **Figure 3-10.** Initially, a pre-shearing at a rate of 150 s^{-1} was applied for 75 s to ensure a similar shear history for all the tested cement pastes. The flow curve was then proceeded by applying a stepped down-curve protocol (to avoid thixotropic effect) at shear rates of 150, 100, 80, 60, 40, 20, 10, 1, 0.1 rotation per s [73]. Different step duration was considered ranging from 15 to 30 s to reach equilibrium. Cement paste has a nonlinear flow behavior, therefore, Modified Bingham (MB) (**Eq. 3-1**) and Herschel-Bulkley (HB) (**Eq. 3-2**) models were used for fitting the data as they are most recommended in the literature [74], [75]. However, the MB model was reported in Section 4.2.4 as it provided a better fit.

$$\tau = \tau_0 + \mu\dot{\gamma} + c\dot{\gamma}^2 \qquad \textbf{Eq. 3-1}$$

$$\tau = \tau_0 + K\dot{\gamma}^n \qquad \textbf{Eq. 3-2}$$

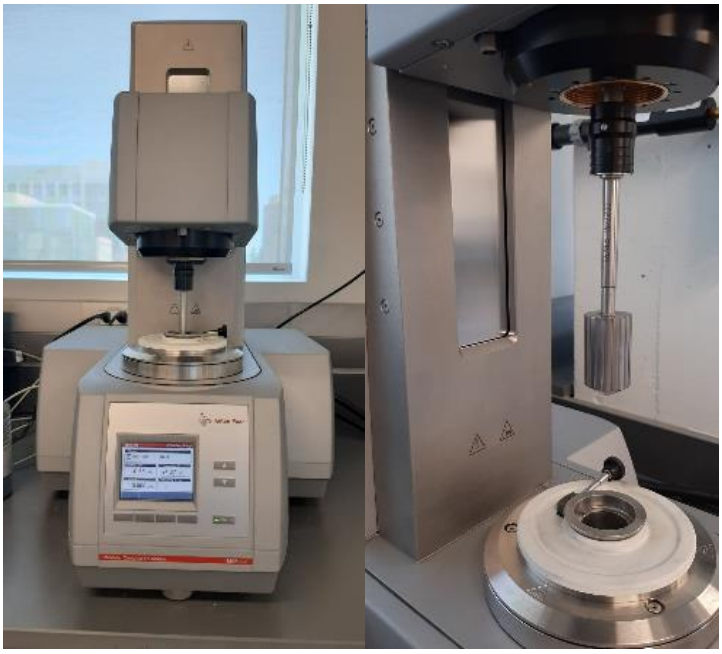

Figure 3-9: Photograph of the rheometer used in this study.

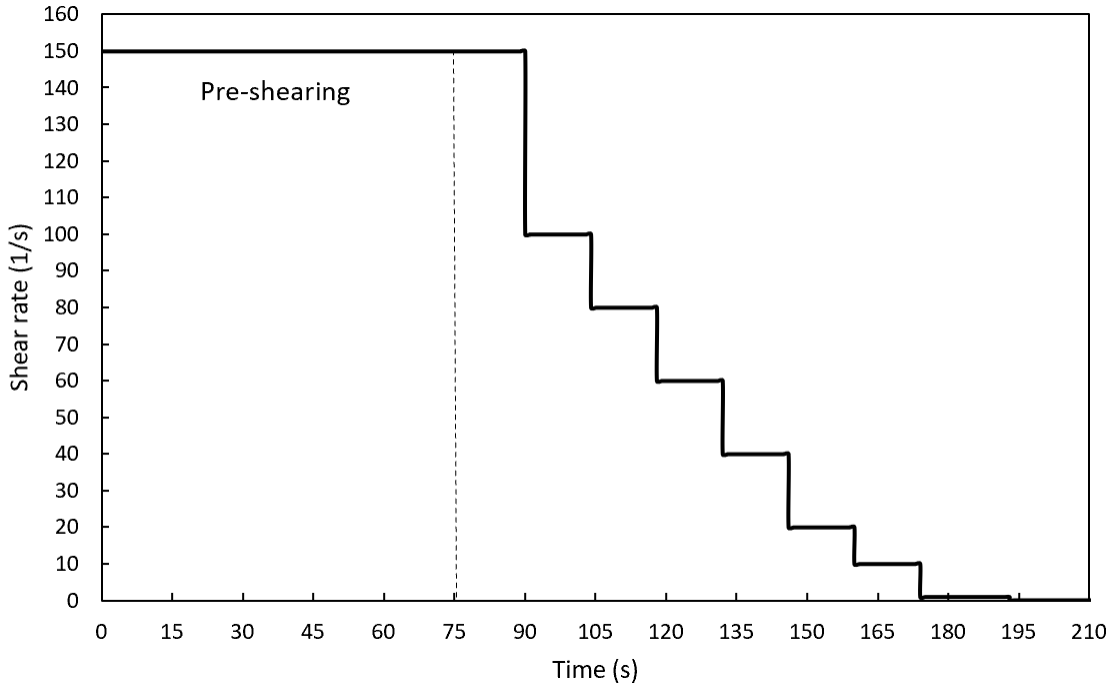

Figure 3-10: Schematic diagram of the protocol used for the flow curve test.

4 Chapter 4: Results and Discussion

4.1 Characterization of Nanosilica Samples

TEM images of synthesized nanosilica samples with different particle sizes are shown in **Figure 4-1**. As seen, all the nanosilica samples had smooth and spherical shapes. Image analysis revealed that N1 to N4 nanosilica particles had an average size of 11±3, 34±9, 66±17, and 92±18 nm. The size distribution of these particles is provided in Appendix B. While the average size of N4 was 92 nm, which falls within the nanorange, some particles in this sample exceeded 100 nm.

N5 had an average particle size of 108 nm based on DLS, therefore, it was not considered for further investigation. The average sizes of the nanosilica samples were rounded to their nearest five and labelled with the notations of NS10, NS35, NS65, and NS90, respectively. Moreover, comparing the results of TEM analysis and DLS measurements (**Table 3-2**) confirms that the particle size findings were closely aligned. It is worth mentioning that the negative zeta potential measurements for these samples also confirm its stability in aqueous solution (**Table 3-2**).

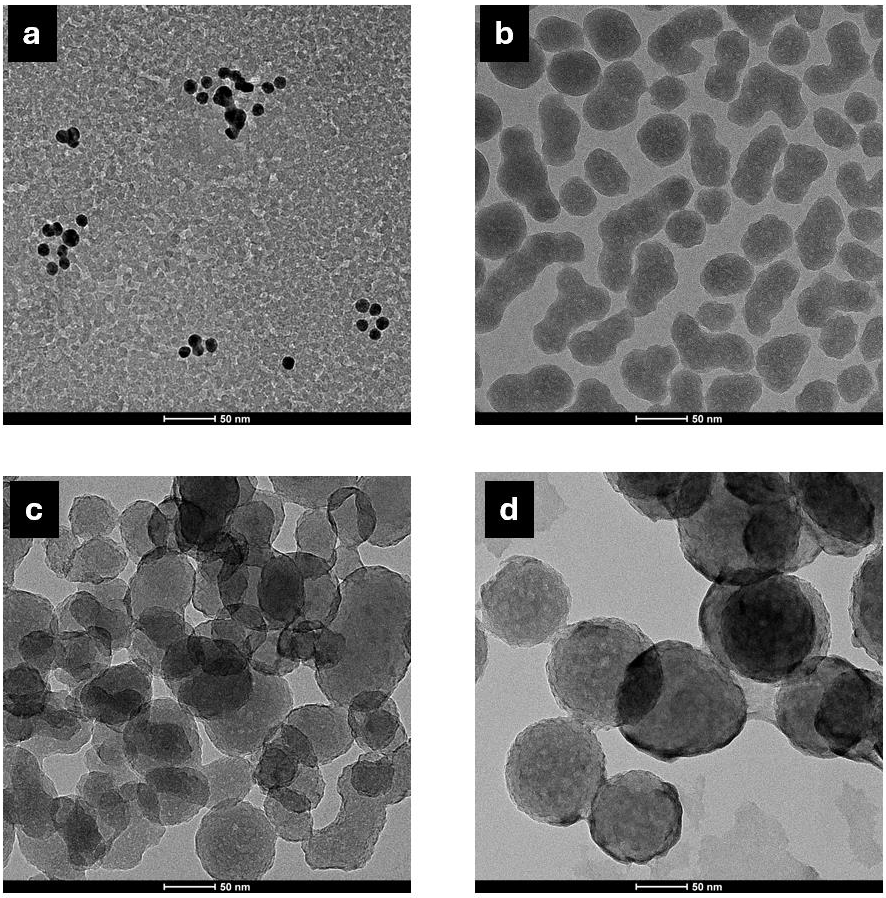

Figure 4-1: TEM images of nanosilica samples, a) NS10, b) NS35, c) NS65, and d) NS90.

XRD patterns and FTIR spectra of the nanosilica samples are depicted in **Figure 4-2** and **Figure 4-3**, respectively. A broad peak was observed in the XRD patterns which was attributed to SiO_2 (JCPDS no. 00-013-0026) [76]. In crystalline materials, XRD patterns show sharp, well-defined peaks corresponding to the regular arrangement of atoms. However, for amorphous materials, the atoms are arranged randomly, leading to broad rather than sharp peaks. The lack of sharp peaks in the XRD patterns of the synthesized nanosilica samples indicates their amorphous structures. This amorphous structure is favorable for their application in cementitious mixtures as they can offer a higher pozzolanic reactivity [77].

In the FTIR spectra of nanosilica samples, the bands at 3605, 1597 and 785 cm^{-1} are due to the stretching of O-H groups and water molecules retained onto the silica surface [78], [79], [80]. A band at the wavenumber of 2330 cm^{-1} was attributed to the Si-H stretching [81]. The strong Si–O–Si stretching band was observed at ~1084 cm^{-1} [81] for all nanosilica samples and the band at ~923 cm^{-1} was attributed to Si–OH vibration [82]. Overall, the structural consistency among all nanosilica samples was evident from the FTIR spectra. XPS survey results for the nanosilica samples are shown in **Figure 4-4**. The results confirm that silicon and oxygen atoms were mainly present at the surface of all the nanosilica samples.

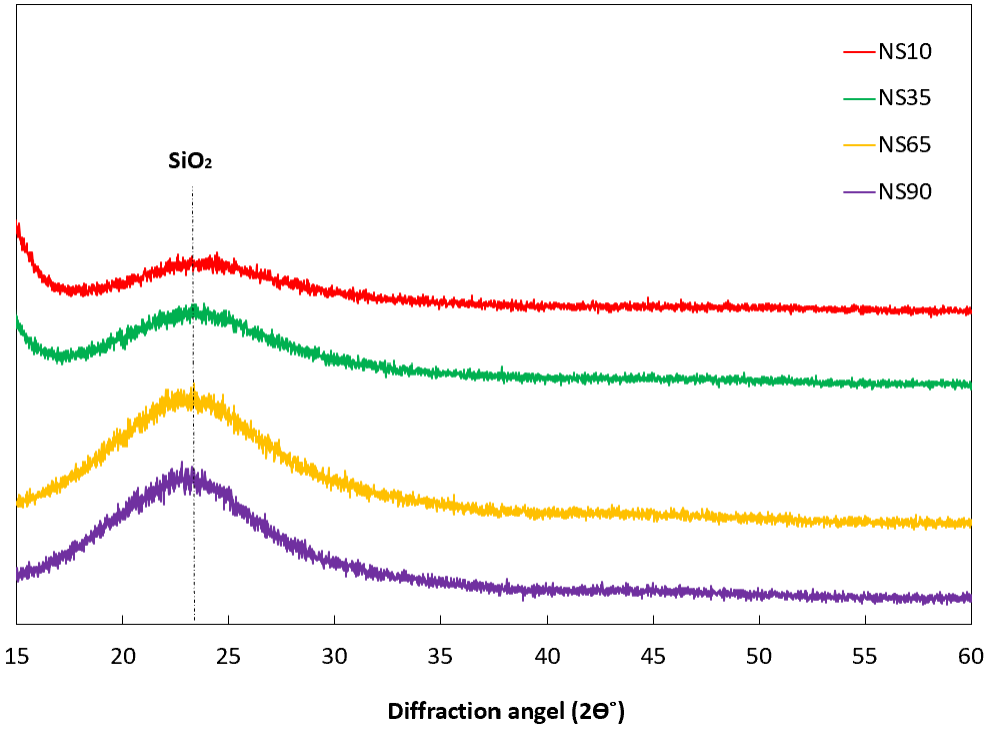

Figure 4-2: XRD patterns of nanosilica samples with different particle sizes.

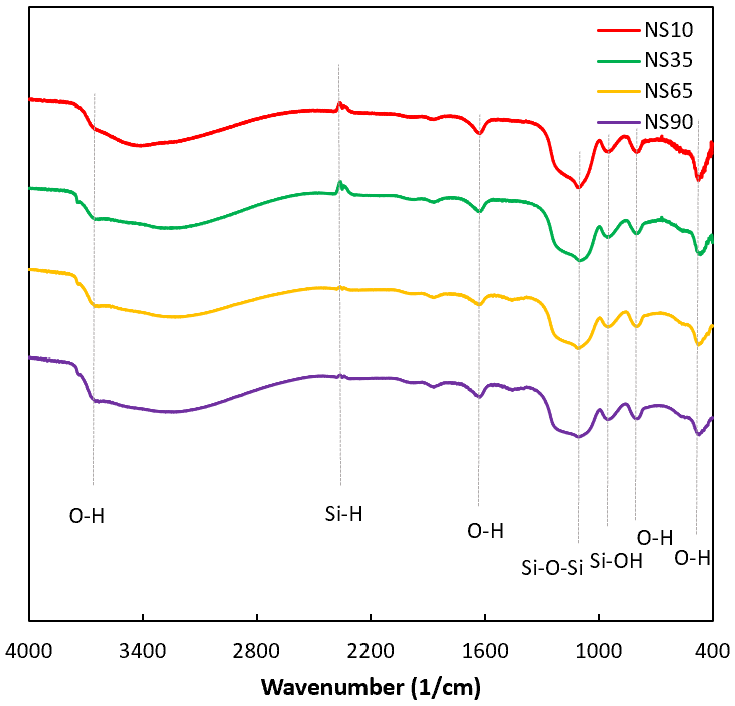

Figure 4-3: FTIR spectra of nanosilica samples with different particle sizes.

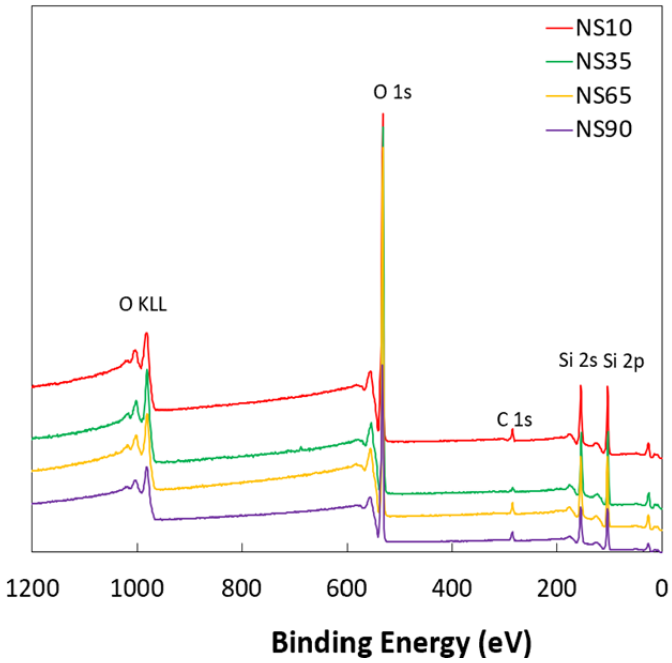

Figure 4-4: XPS survey spectra of nanosilica samples with different particle sizes.

4.2 Properties of Cement Paste

4.2.1 Compressive Strength

Compressive strength measurements at 7, 28 and 91 days for the reference cement paste and pastes incorporating 1 wt% nanosilica with different particle sizes are shown in **Figure 4-5**. The error bar in these figures represents the standard deviation of seven cement pastes that were tested for compressive strength at each age. In general, the addition of nanosilica particles increased the compressive strength of the cement pastes at all testing ages. For example, adding 1 wt% NS10 (nanosilica with a mean particle size of ~10 nm) increased the compressive strength of the cement paste by almost 40% at the age of 7 days. The enhancing effect of the nanosilica particles became less pronounced as their particle size increased such that NS35, NS65, and NS90 increased the 7-day compressive strength of the pastes by 28%, 17%, and 10%, respectively. At later ages (28 and 91 days), the enhancing effect of the nanosilica particles with smaller particle sizes (NS10 and NS35) remained relatively similar to that observed at the earlier age, while higher improvements in the compressive strength of the pastes were observed with larger nanosilica particles (NS65 and NS90) as time elapsed. This is likely because smaller nanosilica particles can react faster and deplete more quickly within the cement paste compared to larger ones. The maximum enhancing effect of NS65 and NS90 on the compressive strength of the pastes was observed at the age of 91 days, with an increase of 37% and 27%, respectively, compared to the reference paste. Compressive strength enhancement of cement pastes with NS65 at 91 days approached that of the paste with the smallest nanosilica particles (NS10). However, the enhancing effect that was observed due to the incorporation of NS90 was still lower than that achieved by the other nanosilica samples by at least 10%.

The enhancing effect that was observed in this research was comparable and even higher (with NS10) than that reported in the literature for 1 wt% concentration of nanosilica in cement paste. Kim and Moon [84] observed less than 10% improvement with 14 nm nanosilica particles in cement pastes at 7 and 28 days. In contrast, Chen et al. [85] reported an approximately 40% improvement in compressive strength using superhydrophobic nanosilica at 7 days, although they did not provide any information about the particle size of their nanosilica or the 28-day strength measurements. Xiao et al. [60] found approximately 40% compressive strength enhancement in cement pastes at 7 days when using nanosilica with 15 and 30 nm particle size, which was reduced to less than 30% improvement at 28 days. On the other hand, in the literature, it is debated whether smaller nanosilica particles are more effective than larger ones at enhancing the compressive strength of cementitious mixtures. Some literature claimed that the optimal compressive strength enhancement of cementitious mixtures with nanosilica particles occurred with larger sizes, such as 20, and 40 compared to sizes of 7 and 12, respectively [53], [56] . Bolhassani et al. [53] used high speed mixing for 5 min to disperse the nanosilica particles in the cement paste while Maagi et al. [56] used dispersant in the mixture, although they did not provide any information about the type and amount of dispersant. These studies suggested that poor dispersion of smaller nanosilica particles could be the reason behind their findings although they did not provide any experimental analysis to quantify the dispersion of nanosilica in the mixtures. However, it appeared that the synthesized method used in our study successfully overcame these drawbacks, revealing the higher potential of smaller nanosilica particles in enhancing the compressive strength of cement paste at different testing ages.

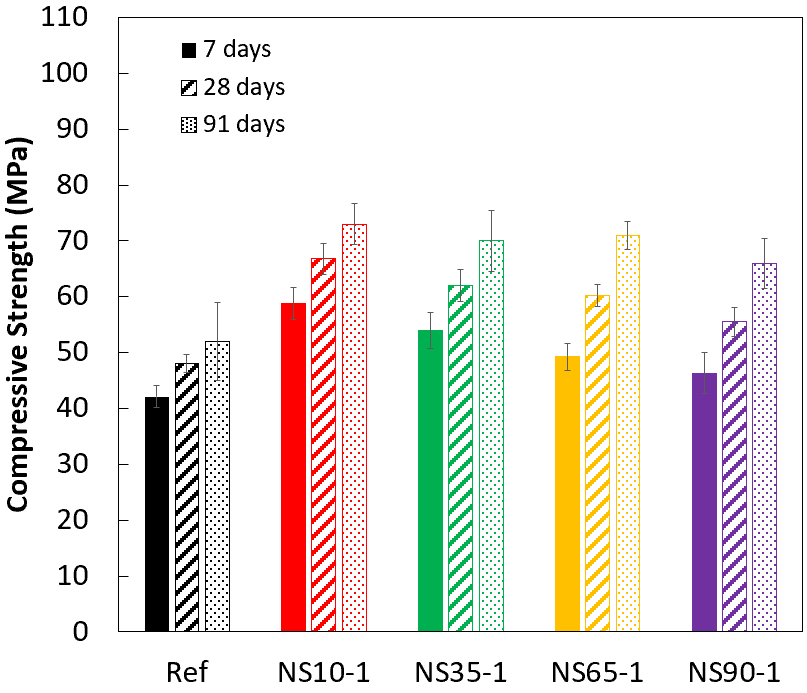

Figure 4-5: Compressive strength of cement pastes at 7 days (solid color), 28 days (dash color), and 91 days (point color) with 1 wt% incorporation of nanosilica with different particle sizes compared to the reference paste.

Compressive strength measurements for cement pastes incorporating 2 wt% nanosilica with different particle sizes as compared to the reference paste are shown in **Figure 4-6**. A comparison of **Figure 4-5** and **Figure 4-6** showed that the enhancing effect of all nanosilica particles was considerably higher when the concentration of nanosilica increased from 1 wt% to 2 wt%. The addition of 2 wt% NS10, for example, increased the 7-day compressive strength of the paste from 42 MPa to 80 MPa, representing 90% enhancement compared to the reference paste. This enhancing effect was even slightly higher at later ages (28 and 91 days) and surpassed 100%. This significant enhancement with NS10 exceeded the reported data in the literature for the enhancing effects of nanosilica even when used at higher concentrations [39], [86], [53]. Nanosilica particles with larger sizes (N35, N65, and N90) were less effective in enhancing the compressive strength of the cement paste compared to NS10; however, they still showed significant improvements

compared to the reference paste at all testing ages. The addition of NS35 at 2 wt% resulted in approximately 40% increase in compressive strength at 7 days, followed by enhancements of about 30% for NS65 and 15% for NS90, compared to the reference paste. This enhancement further increased to 50%, 40% and 25% for NS35, NS65 and NS90, respectively at 28 days compared to the reference paste. It is worth noting that, at 91 days, the compressive strength of cement pastes with NS65 and NS90 was still about 10% less than the 7-day compressive strength of the paste with NS10. These trends highlight the efficacy of using smaller size nanosilica particles in enhancing the compressive strength of cement paste compared to larger ones. Such significant enhancements can be particularly beneficial for structural applications where high compressive strength is needed.

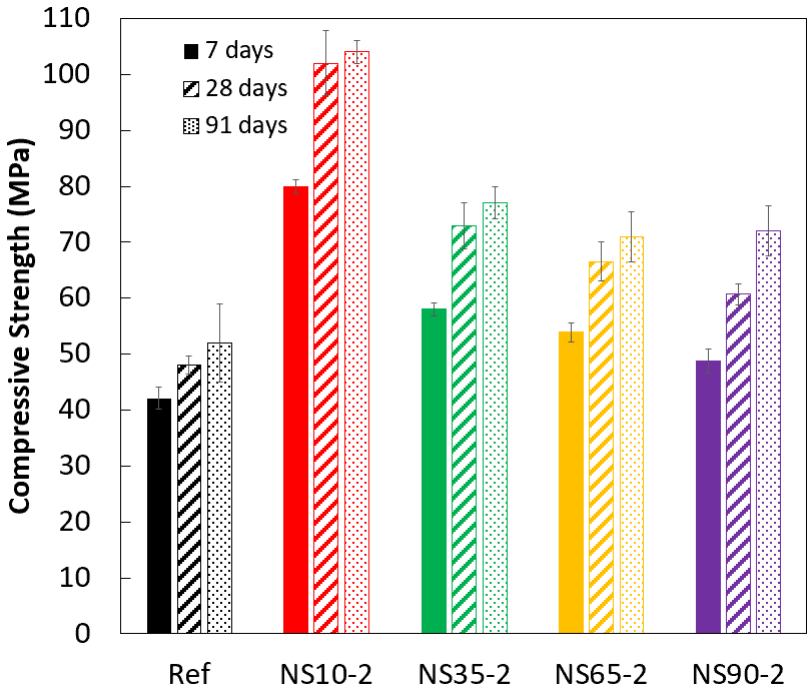

Figure 4-6: Compressive strength of cement pastes at 7 days (solid color), 28 days (dash color), and 91 days (point color) with 2 wt% incorporations of nanosilica with different particle sizes compared to the reference paste.

The effect of incorporating 3 wt% nanosilica on the compressive strength of cement pastes is shown in **Figure 4-7**. Similar to what was observed at lower nanosilica concentrations, the highest compressive strength enhancement with 3 wt% incorporation of nanosilica was achieved with NS10 at 7, 28 and 91 days. Increasing the concentration of nanosilica particles from 2 wt% to 3 wt% for NS35, NS65, and NS90 improved their enhancing effect on the compressive strength of cement pastes at all testing ages. In contrast, cement pastes with NS10 showed almost the same compressive strength enhancement compared to 2 wt% at the age of 28 and 91 days. This enhancement was even 20% less than that in cement paste with 2 wt% incorporation of NS10 at 7 days. This result agrees with those reported by Khan et al. [64] suggesting that nanosilica with smaller particle size (1-3 nm) showed the highest compressive strength enhancement at the lowest concentration (0.5 wt%), while larger particles (35-75 nm) showed their highest enhancement at higher concentrations (5 and 10 wt%) in mortar samples. They reported that this effect likely occurred as smaller nanosilica particles dispersed more effectively at lower concentrations, which likely enhanced their pozzolanic reaction and increased the amount of C-S-H in the mixtures [64].

Comparing the compressive strength results of adding 1, 2, and 3 wt% of nanosilica with various particle sizes to cement pastes suggests that the optimal concentration for NS10 was 2 wt%. NS35, NS65, and NS90, however, were still effective in enhancing the compressive strength of the pastes at 3 wt%. It is suggested based on the comparison of **Figure 4-5** to **Figure 4-7** that the compressive strength enhancement that was achieved with the addition of 1 wt% NS10 could also be achieved by using larger nanosilica particles at higher concentrations. However, the enhancing effect of 2 wt% NS10 on the compressive strength of the pastes was not achieved by other nanosilica particles even when they were used at 3 wt%. It is worth noting that the mixing of cement pastes became significantly more difficult when the concentration of nanosilica particles

was increased from 2 wt% to 3 wt%. This was also evident by the rheological measurements of cement pastes that will be discussed in Section 4.2.4. Therefore, increasing the nanosilica concentration beyond 3 wt% without the use of any superplasticizer may not be feasible in terms of the constructability of these mixtures.

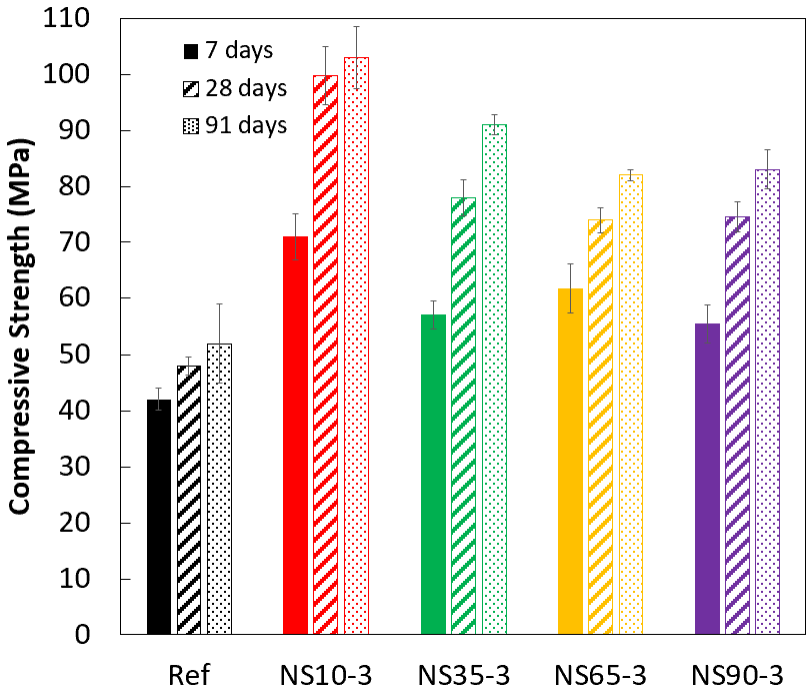

Figure 4-7: Compressive strength of cement pastes at 7 days (solid color), 28 days (dash color), and 91 days (point color) with 3 wt% incorporations of nanosilica with different particle sizes compared to the reference paste.

4.2.2 Heat Evolution

The normalized heat flow of cement pastes incorporating 1 wt% nanosilica as compared to the reference paste is presented in **Figure 4-8**. The key observations such as acceleration period, main peak of heat flow along with the cumulative heat at 1, 3, and 7 days are summerized in **Table 4-1**. The method that was used for calculation of acceleration period is described in Appendix C.

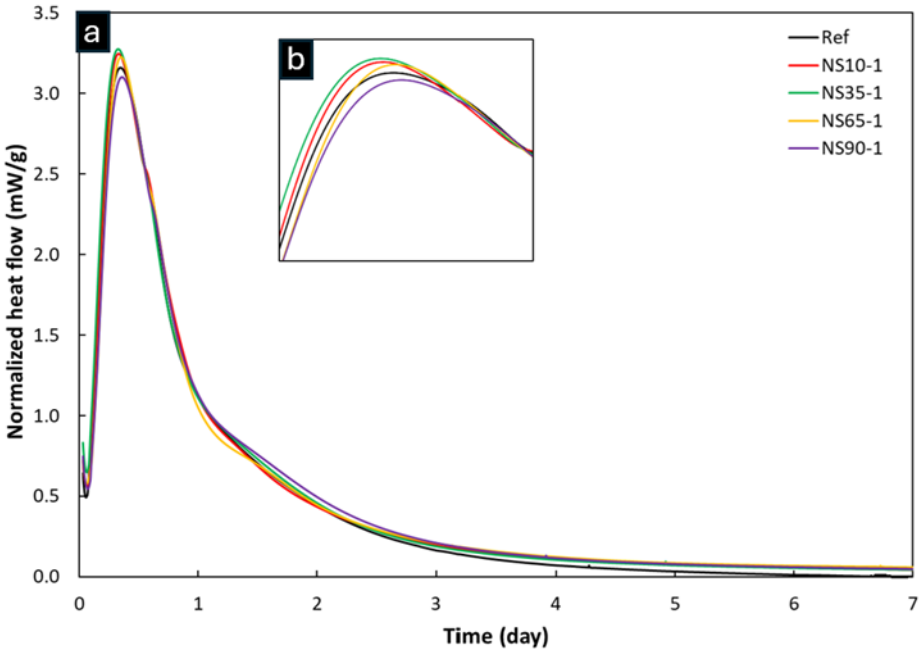

Figure 4-8: a) Normalized heat flow for cement pastes with 1 wt% nanosilica with different particle sizes compared to the reference paste, b) The inset shows the enlarged section of the heat flow peak.

Table 4-1: Key observations of the normalized heat flow and cumulative heat curves for the reference paste and cement pastes with different particle sizes and concentrations of nanosilica.

	Acceleration period (h)	**Main peak of norm. heat flow (mW/g)**	**Norm. cum. heat 1 day (J/g)**	**Norm. cum. heat 3 days (J/g)**	**Norm. cum. heat 7 days (J/g)**
Ref	6.1	3.2	169.4	256.1	272.3
NS10-1	5.7	3.2	174.2	261.3	291.0
NS35-1	5.9	3.2	174.8	265.0	292.0
NS65-1	5.9	3.2	169.2	256.0	289.1
NS90-1	6.2	3.1	167.6	262.1	292.9
NS10-2	5.3	3.8	187.4	264.5	290.0
NS35-2	5.1	3.6	182.2	266.4	291.0
NS65-2	5.7	3.4	174.2	254.7	281.3
NS90-2	6.2	3.1	167.5	260.8	281.0
NS10-3	6.0	2.7	150.5	232.5	265.5
NS35-3	6.0	3.1	169.5	260.0	291.2
NS65-3	6.2	2.9	159.2	247.6	283.5
NS90-3	6.2	3.0	160.9	252.8	289.7

The initial hydration heat flow peak, emerging after the induction period, is associated with the formation of C-S-H resulting from cement hydration [87]. As shown in **Figure 4-8**, the incorporating 1 wt% nanosilica of different sizes in cement pastes did not significantly change the magnitude of this peak. However, this exothermic peak occurred more rapidly, shifting the peak location to earlier times for the pastes with 1 wt% nanosilica of NS10, NS35 and NS65. The use of 1 wt% NS90, however, did not significantly affect the acceleration period of cement pastes. The cumulative heat generated for cement pastes with NS10 and NS35 surpassed that of the reference paste at all the ages (1, 3, and 7 days). For NS65 and NS90, the cumulative heat was initially lower than that of the reference paste, however, eventually exceeded it by 7 days. Both accelerated cement hydration and nanosilica pozzolanic reaction are exothermic reactions that can contribute to the total accumulative heat generation. However, further analysis is required to distinguish between the two mechanisms.

The normalized heat flow of cement pastes with 2 wt% nanosilica compared to the reference paste is shown in **Figure 4-9**. With increasing the concentration of nanosilica particles from 1 wt% to 2 wt% in cement pastes, the difference between the heat flow peak in nanosilica incorporated cement pastes and the reference paste became more pronounced. As illustrated in **Figure 4-9** and **Table 4-1**, the highest heat flow peak was observed in the cement paste containing NS10, which was 20% higher than that of the reference paste. This was followed by NS35 with a 13% increase, and NS65 with a 6% increase compared to the reference paste. However, the cement paste with NS90 did not exhibit a higher heat flow peak compared to the reference paste.

Smaller nanosilica particles (NS10 and NS35) demonstrated a greater acceleration effect on cement hydration, reducing the acceleration period by about 50 and 60 minutes compared to the reference paste. As the size of the nanosilica particles (NS65 and NS90) increased, the cement

pastes exhibited a longer acceleration period compared to the pastes incorporating smaller nanosilica particles, although the acceleration period was still shorter or comparable to that of the reference paste in NS65-2 and NS90-2. This could be due to the nucleation effect of nanosilica particles which leads to faster hydration of the Portland cement. The cumulative heat at the end of 1 day for all the cement pastes with 2 wt% nanosilica particles was higher than that of the reference paste, except for NS90, which was comparable to the reference paste. However, by 7 days, the cumulative heat of NS90-2 also exceeded that of the reference paste. It is worth noting that high heat release of cementitious mixtures can cause thermal gradient and increase the risk of thermal cracking in industrial concrete applications, especially in mass concrete. This can be mitigated by adjustments in the concrete mix design parameters, placement and curing practices. For example, the use of supplementary cementitious materials, such as fly ash and slag, in partial replacement for Portland cement not only reduces the heat release but also has the potential to lower the carbon footprint and other environmental impacts associated with the concrete production.

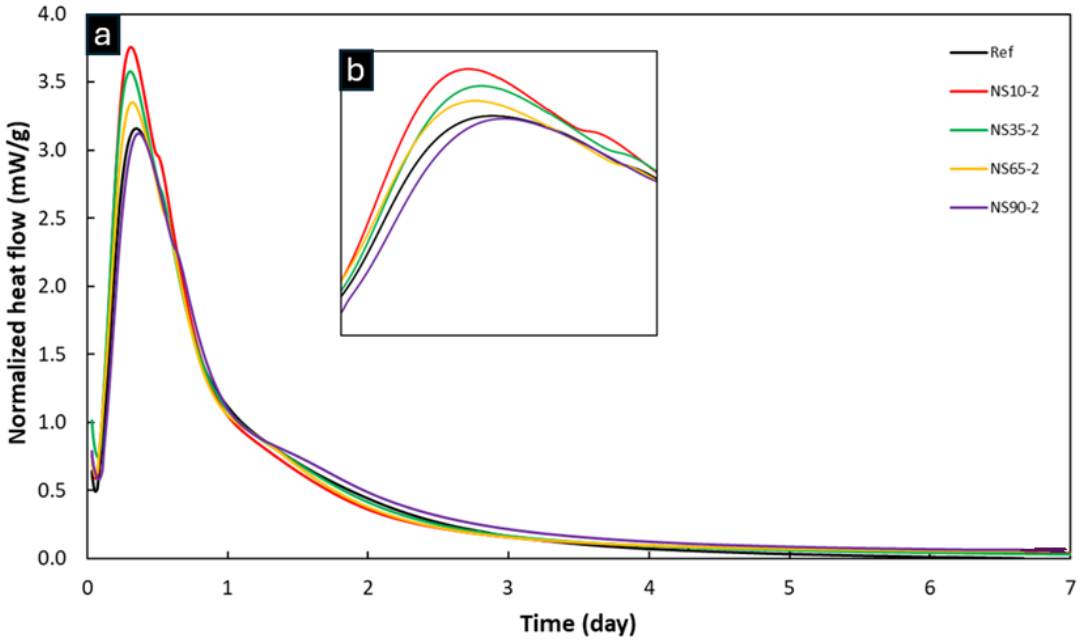

Figure 4-9: a) Normalized heat flow for cement pastes with 2 wt% nanosilica with different particle sizes compared to the reference paste, b) The inset shows the enlarged section of the heat flow peak.

The intensity of the main heat flow peak in cement pastes was reduced or remained unchanged when adding 3 wt% nanosilica particles of different particle sizes (**Figure 4-10**). However, this addition did not significantly affect the acceleration period, with the peak occurring at a similar time compared to the reference paste. The cumulative heat for cement pastes was lower than that of the reference paste at 1 day, with NS10 showing the least amount of heat release. As time progressed to 7 days, the cumulative heat for all cement pastes, except that incorporating NS10, exceeded that of the reference paste. It is possible that the energy used for mixing the cement paste with 3 wt% NS10 was insufficient to effectively disperse the particles in this paste. As a result, some clusters of nanosilica particles may have formed, trapping water within them and reducing the water available for cement hydration. Over time, as the nanosilica particles gradually dissolved, the trapped water was released, contributing to further cement hydration [54], [86]. This

effect on the cement hydration was further discussed in Section 4.2.3 where the QXRD results for 3 wt% nanosilica incorporated samples are described.

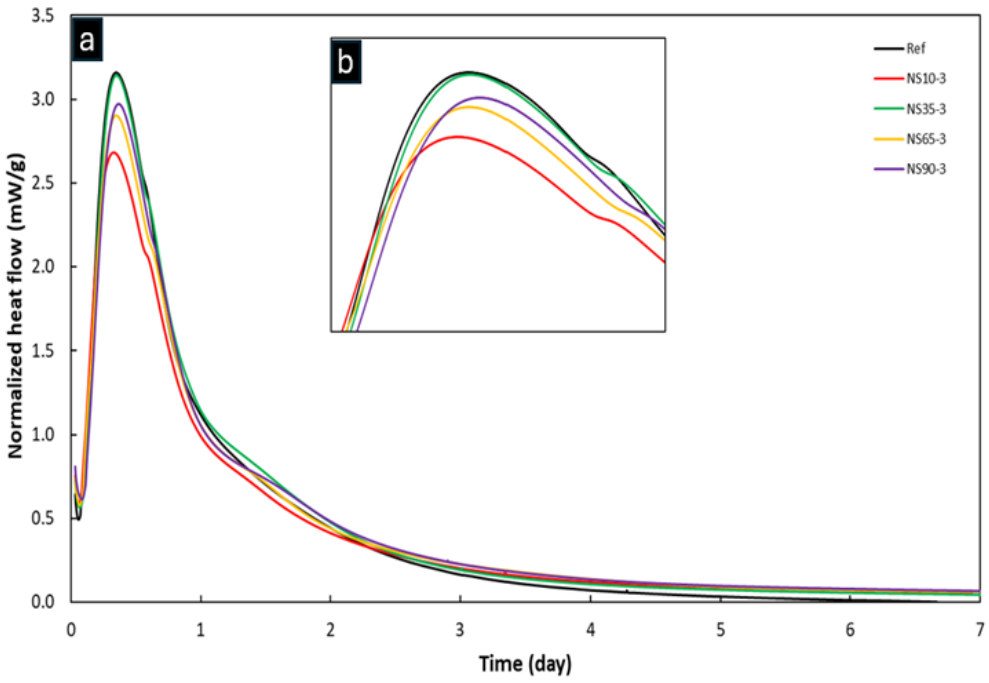

Figure 4-10: a) Normalized heat flow for cement pastes with 3 wt% nanosilica with different particle sizes compared to the reference paste, b) The inset shows the enlarged section of the heat flow peak.

In the existing literature on the effect of nanosilica particle size on heat evolution of cementitious mixtures, Bai et al. [48] reported that cement paste containing 0.9 wt% nanosilica with 20 nm particle size showed higher heat flow peak compared to those in cement paste with 50 nm nanosilica particles. However, the smaller size nanosilica prolonged the acceleration period by approximately 2 hours compared to the reference paste. This finding aligns with our research on the effect of smaller particle sizes at 1 and 2 wt% on the main heat flow peak, however, contradicts our observations regarding the effect of nanosilica particle size on reducing the acceleration period of cement paste. In their research, Bai et al. [48] utilized nanosilica in a powder form which was

dispersed in deionized water by using a sonication bath for 3 h, although they did not mention any information about the portion of the water that was used. However, it was not reported if the sonication was effective in dispersing the nanosilica particles. There are reports that if the sonication is too intense or prolonged, it can cause the particles to re-agglomerate or form new clusters due to the excessive energy input. This can lead to uneven dispersion and the formation of larger, less reactive clusters [88].

4.2.3 Microstructure

The amount of calcium hydroxide (CH) normalized to the dry weight of anhydrous cement [70], as obtained by TGA, for the reference paste and cement pastes with 2 wt% nanosilica at 1, 7, and 28 days is presented in **Figure 4-11**. Among the three different concentrations of nanosilica particles in the cement pastes, 2 wt% was selected for the TGA analysis as it demonstrated the highest improvement in compressive strength and heat flow peak across all tested cement pastes. As expected, the CH content in the reference paste increased through time due to the continued cement hydration. However, no monotonic trend was observed in cement pastes incorporating nanosilica due to the competing effects of two mechanisms on the CH content: accelerated cement hydration that increases the rate of CH formation, pozzolanic reaction of nanosilica particles that consumes CH.

At 1 day, the lowest amount of CH belonged to the cement paste incorporating the smallest nanosilica particles (NS10). Such a low CH content despite the accelerated cement hydration, that was evident by the isothermal calorimetry result as discussed in Section 4.2.2, shows the CH consumption due to pozzolanic reaction of NS10 by this age. At 7 days, the CH content in cement paste with NS10 increased significantly compared to 1 day, suggesting that the rate of CH production due to cement hydration exceeded the rate of CH consumption from the pozzolanic

reaction. The sharp decrease in the CH content of this paste from 7 to 28 days indicates that the amount of CH that was consumed due to pozzolanic reaction is higher than that formed due to the cement hydration during this time.

Cement pastes incorporating nanosilica with larger particle sizes also showed the same trend of increasing and then decreasing the CH content from 1 to 7 and then to 28 days. All of these pastes had higher CH contents compared to NS10 at 1 and 28 days. Cement pastes incorporating NS35 and NS65 showed accelerated cement hydration, as indicated by the isothermal calorimetry data, although it was not as significant as the effect of NS10. Therefore, the higher CH content in these pastes at 1 day compared to that in the paste incorporating NS10 may suggest a lower pozzolanic reactivity of these nanosilica particles in the pastes at this age.

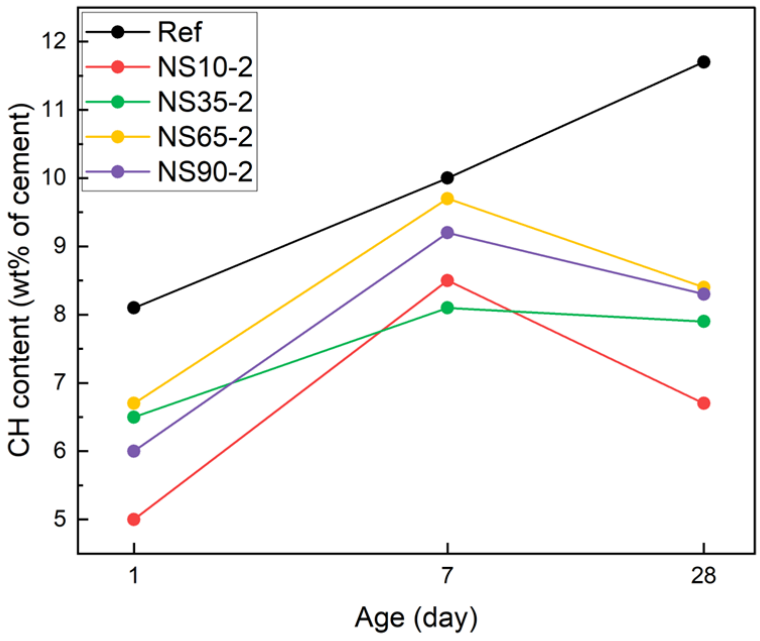

Figure 4-11: CH content normalized to anhydrous cement weight as a function of age for the reference paste and pastes with 2 wt% nanosilica of different particle sizes.

The results of QXRD analysis on the 1-, 7- and 28-day cement pastes with 2 wt% nanosilica with different particle sizes compared to the reference paste are shown in **Table 4-2**. The XRD patterns of these pastes are also provided in Appendix D. Based on the QXRD results, the amount of clinker phases decreased in the reference paste over time. This was expected due to progress in the hydration of cement clinker phases. As a result, higher contents of reaction products including portlandite (CH) and amorphous content, primarily composed of C-S-H, were also formed.

The cement paste with 2 wt% NS10 had lower amount of anhydrous silicate phases (i.e., C_3S and C_2S) compared to the reference paste at 1 day, indicating accelerated hydration of these phases in the cement paste with NS10. This accelerated cement hydration aligns with the data obtained by the isothermal calorimetry (Section 4.2.2). Moreover, the cement paste with NS10 showed approximately 60% more amorphous content compared to the reference paste at 1 day. Despite such a greater degree of cement hydration in the cement paste with NS10, the CH content was lower in this paste than that in the reference paste, suggesting the pozzolanic reaction of NS10 as early as 1 day. From 1 day to 7 days, a sharp decline in the anhydrous C_3S content was observed, while the amount of anhydrous C_2S remained unchanged from 1 day in this cement pastes. Consequently, the amorphous phase in this paste increased from approximately 55% to 67%, which was 30% higher than that of the reference paste at 7 days. By 28 days, both anhydrous C_3S and C_2S contents decreased significantly compared to 7-day values in this paste. As a result, the amorphous content increased to 72.1% which was around 30% more than the amorphous content in the reference paste at the same age. Despite the higher degree of hydration of silicate phases at 28 days compared to 7 days, the CH content decreased. This is consistent with the TGA results

and indicates that CH consumption due to the pozzolanic reaction was more than CH production as a result of cement hydration during this time.

At 1 day, the cement paste incorporating 2 wt% NS35 also had a higher degree of hydration of silicate phases, higher amorphous content, and lower CH content compared to the reference paste. A comparison of the QXRD results for this paste and that incorporating the same concentration of NS10 suggests that the pozzolanic reactivity of NS35 was lower than that of NS10 although it appears that NS35 had greater accelerating effect on the hydration of C_3S compared to NS10. This was also evident in the isothermal calorimetry results that showed a shorter acceleration period for NS35-2 compared to NS10-2. However, further research is required to determine the mechanisms of this behavior. At 7 and 28 days, NS35 still caused accelerated cement hydration and participated in pozzolanic reaction that resulted in a higher amorphous and a lower CH content compared to the reference paste. At 28 days, the amorphous content in the cement pastes incorporating 2 wt% NS35 was close to that in the paste with 2 wt% NS10.

The QXRD results of **Table 4-2** also show that NS65 and NS90 at 2 wt% also accelerated cement hydration and participated in pozzolanic reaction, however, both mechanisms occurred at much a lower rate compared to the NS10 and NS35. The amorphous content of the pastes incorporating 2 wt% NS65 and NS90 were similar at the age of 28 days and was about 25% higher than that in the reference paste but around 6% lower compared to that in the pastes with 2 wt% NS10 or NS35.

Overall, the QXRD analyses suggest that both the accelerated cement hydration and the pozzolanic reaction occurred in the cement pastes incorporating 2 wt% of nanosilica with different particle sizes, however, their rates decreased as the nanosilica particle sizes increased from ~10 to 90 nm. This explains the higher compressive strengths observed for the 2 wt% nanosilica

incorporated cement pastes compared to the reference paste and the fact that this enhancement was higher for the nanosilica with smaller particle sizes compared to larger ones. The other factor that likely contributed to the strength enhancement of cement pastes with nanosilica is the modification of the microstructure in these pastes. We performed scanning electron microscopy (SEM) on the reference paste and that made with 2 wt% NS10 (NS10-2) at a late age of 150 days. The results that are presented in Appendix F confirm a denser microstructure for the NS10-2 compared to the reference paste. However, further analysis is required to study the pore structure in the pastes with various concentrations and sizes of nanosilica at different ages and determine its role in the strength enhancements in these pastes.

Table 4-2: QXRD results for reference paste and cement paste with 2 wt% nanosilica of different particle sizes at 1, 7 and 28 days based on wt% of cement paste.

Name	Ref			NS10-2			NS35-2			NS65-2			NS90-2		
	1 d	7 d	28 d	1 d	7 d	28 d	1 d	7 d	28 d	1 d	7 d	28 d	1 d	7 d	28 d
Alite (C_3S)	13.0	4.6	2.3	12.2	3.9	1.4	7.4	2.1	1.3	9.5	3.1	2.5	11.3	3.7	2.3
Belite (C_2S)	11.3	7.7	6.4	5.4	5.5	3.4	6.7	6.6	5.1	7.1	6.3	4.6	7.7	6.8	5.0
Aluminate (C_3A)	0.6	0.4	0.3	1.3	0.1	0.3	0.5	0.0	0.1	1.4	0.3	0.1	1.3	0.2	0.1
Ferrite (C_4AF)	8.1	4.3	3.2	5.5	2.1	1.5	6.0	2.6	1.4	5.6	3.3	1.5	5.9	2.6	1.9
Calcite	11.1	12.0	12.8	7.5	7.6	8.8	7.9	9.5	8.5	6.8	9.9	7.4	8.7	10.3	8.4
Dolomite	4.7	3.9	4.0	1.9	2.6	2.4	4.0	3.7	3.1	3.3	3.2	3.4	2.3	3.5	3.3
Ettringite	6.9	5.2	5.7	4.6	4.4	4.1	4.3	4.0	3.4	4.7	6.2	5.1	4.2	6.5	4.0
Gypsum	0.6	0.4	0.5	0.3	0.4	0.1	0.3	0.4	0.4	0.4	0.3	0.6	0.5	0.6	0.3
Magnesia	2.4	1.6	1.8	1.8	1.1	0.8	1.4	1.4	0.9	1.3	1.8	1.0	1.5	1.65	1.2
Portlandite	7.2	8.4	8.5	4.3	5.1	4.9	6.1	6.2	4.8	6.9	7.4	6.1	5.2	7.0	5.4
Amorphous	34.0	51.5	54.6	55.4	67.2	72.1	55.6	63.5	71.1	52.8	58.3	67.8	51.4	57.0	68.3

The results of QXRD analysis for cement paste with 1, 2 and 3 wt% nanosilica compared to the reference paste at 28 days are shown in **Table 4-3**. The results indicate that by increasing the nanosilica concentration from 1 to 2 wt% in cement paste with NS10, the anhydrous content of C_3S and C_2S decreased substantially, which indicates a higher hydration degree in this cement paste. Despite this accelerated hydration, the CH content was reduced due to the higher pozzolanic reaction in the paste with the higher NS10 content. Additionally, the amorphous content increased from 58% to 72% by increasing the NS10 from 1 to 2 wt%. These findings align with the substantially higher enhancement in the compressive strength of cement paste incorporating 2 wt% NS10 compared to that incorporating 1 wt% NS10. On the other hand, it appears that increasing the NS10 content from 2 to 3 wt% did not cause any further increase in the cement hydration. There was no evidence of further pozzolanic reaction in the paste with 3 wt% NS10 compared to that with 2 wt% NS10 at 28 days either. This can explain the comparable 28-day compressive strength of the pastes with 2 and 3 wt% NS10.

For NS35, the comparable contents of anhydrous silicate phases together with the lower CH content by increasing the concentration of the nanosilica from 2 to 3 wt% can be due the pozzolanic reaction of this nanosilica that contributes to the 28-day strength enhancement as well. In cement pastes with NS65 and NS90, a decrease in the anhydrous C_3S and C_2S contents, along with approximately 6% increase in the amorphous content were observed as the nanosilica concentration increased from 2 to 3 wt%. This trend is consistent with the compressive strength improvement observed in NS65 and NS90 pastes at the higher nanosilica concentration.

Table 4-3: QXRD results for reference paste and cement paste with 1, 2 and 3 wt% nanosilica of different particle sizes at 28 days based on wt% of cement paste.

Name	Ref	NS10			NS35			NS65			NS90		
	-	1wt%	2wt%	3wt%	1wt%	2wt%	3wt%	1wt%	2wt%	3wt%	1wt%	2wt%	3wt%
Alite (C_3S)	2.3	1.8	1.4	1.9	1.4	1.3	1.4	3.9	2.5	1.3	2.5	2.3	2.1
Belite (C_2S)	6.4	7.0	3.4	5.3	5.6	5.1	5.0	5.2	4.6	4.0	5.9	5.0	4.7
Aluminate (C_3A)	0.3	0.0	0.3	0.3	0.0	0.1	0.0	0.0	0.1	0.0	0.6	0.1	0.0
Ferrite (C_4AF)	3.2	2.5	1.5	1.8	2.3	1.4	1.5	3.8	1.5	1.3	2.0	1.9	1.8
Calcite	12.8	11.7	8.8	8.5	11.0	8.5	8.0	9.3	7.4	8.7	9.3	8.4	6.9
Dolomite	4.0	4.6	2.4	2.9	3.5	3.1	2.9	2.2	3.4	2.9	2.1	3.3	2.4
Ettringite	5.7	4.5	4.1	3.2	4.0	3.4	3.6	3.9	5.1	4.3	3.9	4.0	3.0
Gypsum	0.5	0.7	0.1	0.4	0.5	0.4	0.4	0.4	0.6	0.3	0.3	0.3	0.4
Magnesia	1.8	1.6	0.8	1.1	1.3	0.9	0.8	1.0	1.0	1.0	1.3	1.2	1.1
Portlandite	8.5	7.8	4.9	4.1	6.0	4.8	4.3	7.1	6.1	4.9	6.5	5.4	4.7
Amorphous	54.6	57.8	72.1	70.5	64.8	71.1	72.2	63.3	67.8	71.2	65.5	68.3	72.9

4.2.4 Rheology

The flow curve of cement pastes with nanosilica of different sizes compared to the reference paste is shown in **Figure 4-12**. The viscosity and yield stress of these pastes calculated based on the modified Bingham model (MB) are presented in Appendix E. In general, cement paste can present a shear-thinning phenomenon leading to decrease in viscosity with increasing shear rate [89], [75]. The behavior of the pastes remained shear thinning after the addition of nanosilica with any size or concentration. This agrees with the data reported in the literature, as they reported that adding 1.25 wt% nanosilica in cement paste, showed a shear-thinning behavior [90]. The shear-thinning behavior of cement paste is beneficial for transporting and pumping of cementitious mixtures in construction applications. It can help cementitious mixtures remain stable without sedimentation or solid-liquid separation when stationary, yet flow smoothly when subjected to movement such as during pumping [91].

The addition of all nanosilica particles significantly increased the viscosity and yield stress of the cement pastes (See Appendix E). Due to the importance of viscosity in the constructability of cementitious mixtures, the relationship between apparent viscosity and shear rate for all nanosilica-incorporated pastes compared to the reference paste is shown in **Figure 4-13**. It is worth noting that it was not possible to measure the rheological behavior of the cement pastes with 3 wt% NS10 and NS35, due to their high viscosity.

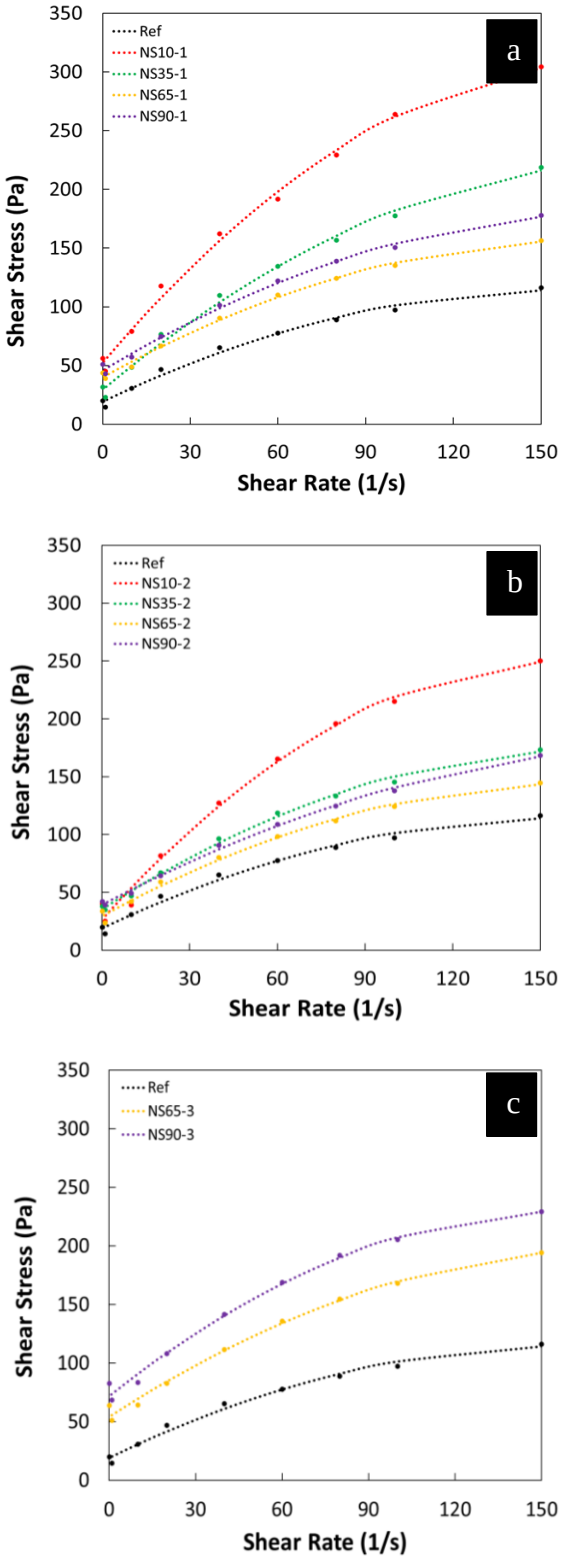

Figure 4-12: Flow curves for cement pastes with a) 1 wt%, b) 2 wt%, and c) 3 wt% nanosilica compared to the reference paste. Points are experimental data, and the dotted lines are from the Modified Bigham Model (Eq. 3-1).

The results of **Figure 4-13 (a)** show that the addition of 1 wt% nanosilica with any of the particle sizes to the cement paste increased the apparent viscosity of the paste at all shear rates. Among all nanosilica particles, NS10 that had the smallest particle size, had the most remarkable effect on the viscosity of the paste, exceeding the viscosity of the paste by more than 100% at shear rates higher than 60 1/s. Other nanosilica particles (i.e., NS35, NS65, and NS90) had less pronounced effects on the viscosity of the paste (i.e., between ~25 to 50% increase).

The apparent viscosity for cement pastes incorporating 2 wt% nanosilica with different particle sizes as compared to the reference paste is shown in **Figure 4-13 (b)**. A comparison of **Figure 4-13 (a)** and **Figure 4-13 (b)** shows that the viscosity of all nanosilica incorporated cement pastes was higher when the concentration of nanosilica increased from 1 wt% to 2 wt%. The viscosity of cement paste with 2 wt% NS10 showed an increase of over 150% compared to the reference paste. Flores et al. [92] reported that the viscosity of cement pastes with nanosilica increased by about 80% when nanosilica (mean particle size of 4 nm) was added at 2.5 wt%. However, they used 0.6 wt% superplasticizer in their mixtures to achieve the flow diameter of 100 to 120 mm while we did not use any superplasticizer in our research. For cement pastes with larger nanosilica particles, the increase in the viscosity was less significant compared to the paste with NS10. The incorporation of NS35 in the cement paste increased its viscosity by ~70-90% compared to the reference paste. This increase was ~35%, and ~50% for cement pastes with NS65 and NS90, respectively.

The effect of incorporating 3 wt% NS65 and NS90 on the viscosity of cement pastes is shown in **Figure 4-13 (c)**. Increasing the concentration of these nanosilica particles from 2 to 3 wt% further increased the viscosity of the cement pastes. Adding 3 wt% nanosilica of NS65,

increased the viscosity of cement paste over 70% compared to the reference paste, while this amount was about 110% for the cement paste with NS90.

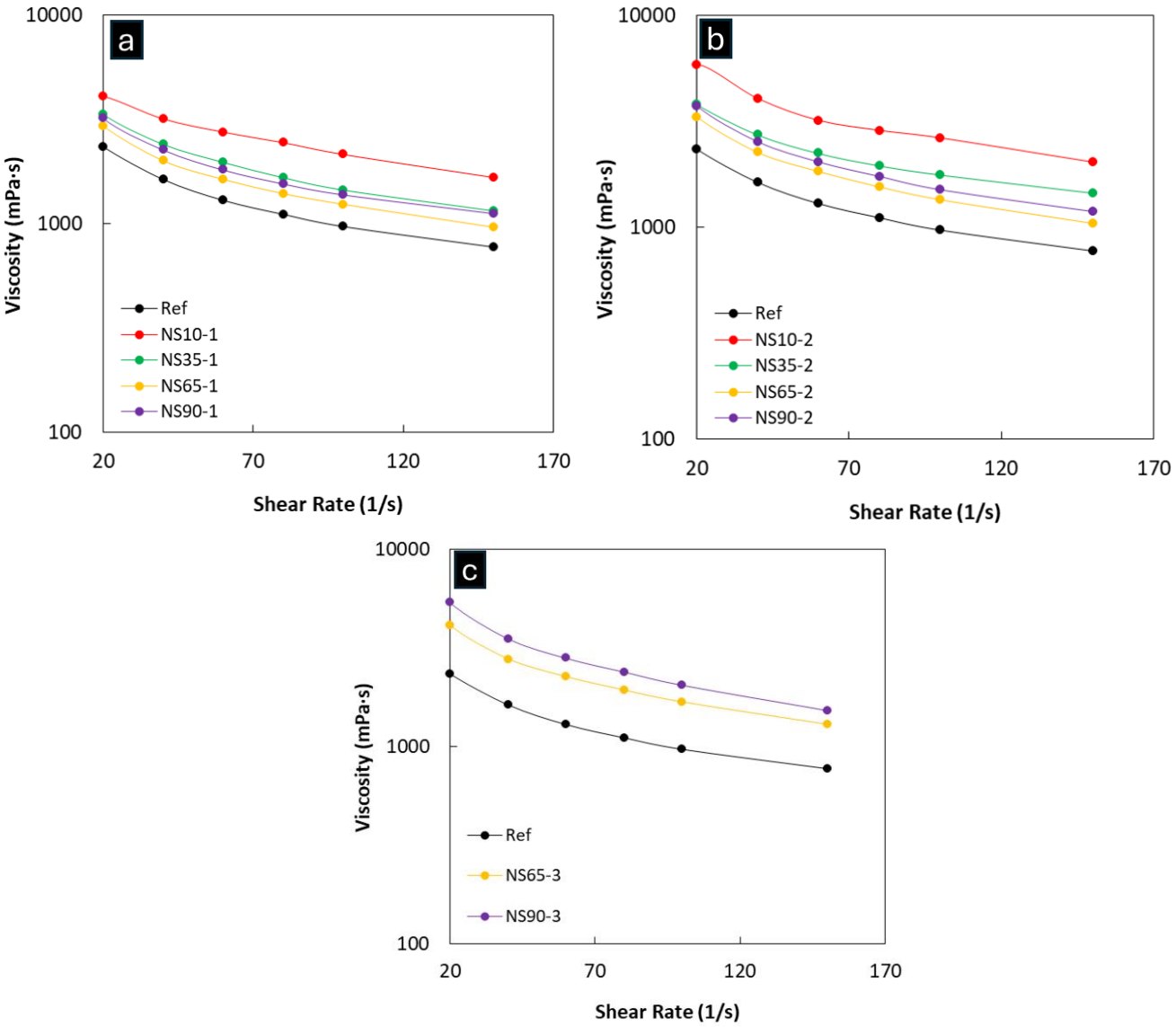

Figure 4-13: Apparent viscosity for cement paste with a) 1 wt%, b) 2 wt% and c) 3 wt% nanosilica compared to the reference paste.

The higher viscosity of cement paste with smaller size nanosilica has also been reported in the literature. Sun et al. [61] reported that addition of 1 wt% nanosilica with the mean particle size of 40 nm increased the viscosity of cement paste ~60% more than addition of the same

concentration of nanosilica with 100 nm particle size. Nanosilica significantly increases the water demand in cement paste due to its high specific surface area. Its surface hydroxyl groups readily adsorb surrounding moisture, creating a microstructure similar to flocculated cement, which further traps water [93]. This effect is more pronounced when the smallest nanosilica particles (NS10) are used, as their large specific surface area allows them to absorb more water, reducing the fluidity of the paste. Consequently, cement pastes with smaller nanosilica particles exhibit higher viscosity compared to those containing larger particles. Similarly, the viscosity of the paste increases with the increase in the concentration of the nanosilica particles. In our study, the viscosity of the cement paste with 1 wt% NS10 and the paste with 3 wt% NS90 were comparable at shear rates greater than 60 1/s.

The viscosity of fresh cementitious mixtures plays an important role in their stability (i.e., resistance to separation of their ingredients) and constructability. While a sufficiently high viscosity is required to prevent the sedimentation of the solid particles in cementitious mixtures, very high viscosity of these mixtures negatively affects their constructability. This was also observed in this study when smaller size nanosilica particles (NS10 and NS35) were used at a high concentration of 3 wt% and these mixtures became difficult to mix. Therefore, if high concentrations of nanosilica, particularly those with very small particle size, need to be used in cementitious mixtures due to the other performance enhancement requirements, such as compressive strength enhancement, the use of superplasticizer and other mix design adjustments may be required.

The ability of nanosilica to increase the viscosity of cementitious mixtures has made it a great candidate for application as a base for viscosity modifying admixtures (VMA) in concrete. That is particularly advantages in self-consolidating concrete (SCC) which poses a high fluidity

and is susceptible to segregation. The effect of nanosilica-based VMAs on the viscosity of cementitious mixtures has been reported in the literature. For example, Leemann et al. [94] compared the effects of different VMAs on the rheology of mortars. They reported that incorporating 1 wt% of a nanosilica-based VMA, which had 16.4% solid content, increased the viscosity by approximately 30% in mortar samples. In our research, the increase in the viscosity of the cement pastes incorporating 1-3 wt% nanosilica with various particle sizes ranged from ~30% to over 150% depending on the size and concentration of the nanosilica. Further investigation is needed to explore the effect of nanosilica particle size on the performance of cementitious mixtures as a VMA.

5 Chapter 5: Conclusions and Recommendations for Future Research

5.1 Conclusions

In this study, nanosilica particles with various particles sizes (i.e., mean particle size of 10, 35, 65 and 90 nm) were synthesized, fully characterized, and then utilized in cement paste in three different concentrations (1, 2 and 3 wt% of cement). The cement pastes incorporating nanosilica particles were tested for compressive strength, heat evolution, microstructure, and rheology. The main concluding remarks are as follows:

- Characterization of the in-house prepared nanosilica particles confirmed their spherical shape and stability in water with control over their size. It also confirmed their amorphous structure and comparable surface chemistry.
- The addition of nanosilica particles had a considerable effect on enhancing the compressive strength of cement paste at different ages. Cement pastes incorporating 2 wt% NS10 showed the highest compressive strength improvement, with over 100% enhancement at the ages of 28 and 91 days. This enhancement surpassed those reported in the existing literature. Nanosilica with larger particle sizes (> 10 nm) still enhanced the compressive strength of cement paste although their enhancing effect decreased as their size increased from 10 to 90 nm at any given concentrations.
- Acceleration of the Portland cement hydration, pozzolanic reaction of the nanosilica, and refining the microstructure of the cement paste all contributed to the enhanced compressive strength of cement paste incorporating nanosilica. At 2 wt%, the nanosilica with the

smallest particle size of ~10 nm showed the highest pozzolanic reactivity and a great ability to accelerate cement hydration compared to other nanosilica particles.

- Nanosilica, particularly NS10, significantly increased the viscosity of cement paste, which can affect the constructability of the mixture, although it can also be advantageous for application as a viscosity-modifying admixture.

5.2 Recommendations for Future Research

Despite the comprehensive study conducted in this thesis on the application of nanosilica with controlled particle sizes for enhancing the performance of cementitious mixtures, there remains significant potential for further research on this topic. Based on the content of this thesis, the following recommendations are suggested for future research:

- Scale up the research scope to include the effects of nanosilica with various particle sizes on the performance of mortar and concrete.
- Study additional performance parameters, including modulus of elasticity, tensile strength, and durability aspects such as water absorption, resistance to chloride penetration, carbonation, and freeze-thaw cycles, and shrinkage.
- Investigate the impact of nanosilica on the pore structure of cementitious mixtures.
- Evaluate the potential of nanosilica particles with various sizes to reduce the Portland cement content in cementitious mixtures without compromising the performance of these mixtures.
- Investigate the effect of nanosilica with various particle sizes in cementitious mixtures made with blended cements, especially those containing large volumes of supplementary cementitious materials, or alternative binders, such as geopolymers.

- Explore the use of nanosilica particles of different sizes as a base for viscosity modifying admixture in cementitious mixtures with tendency for segregation such as SCC.
- Conduct a life-cycle assessment to determine the effect of nanosilica with different particle sizes on the life-cycle cost and environmental impacts of cementitious mixtures in structural applications.

6 References

[1] "Global cement and concrete industry announces roadmap to achieve groundbreaking 'net zero' CO_2 emissions by 2050," GCCA. Accessed: May 02, 2024. [Online]. Available: https://gccassociation.org/news/global-cement-and-concrete-industry-announces-roadmap-to-achieve-groundbreaking-net-zero-co2-emissions-by-2050/

[2] W. Kurdowski, *Cement and Concrete Chemistry*. Dordrecht: Springer Netherlands, 2014. doi: 10.1007/978-94-007-7945-7.

[3] K. Khan, W. Ahmad, M. N. Amin, and S. Nazar, "Nano-silica-modified concrete: A bibliographic analysis and comprehensive review of material properties," *Nanomaterials*, vol. 12, no. 12, p. 1989, 2022.

[4] L. P. Singh, S. R. Karade, S. K. Bhattacharyya, M. M. Yousuf, and S. Ahalawat, "Beneficial role of nanosilica in cement based materials–A review," *Constr. Build. Mater.*, vol. 47, pp. 1069–1077, 2013.

[5] N. Tkachenko *et al.*, "Global database of cement production assets and upstream suppliers," *Sci. Data*, vol. 10, no. 1, p. 696, Oct. 2023, doi: 10.1038/s41597-023-02599-w.

[6] P. Mehta and P. Monteiro, *Concrete: Structure, Properties, and Materials*. 2013.

[7] J. Beaudoin and I. Odler, "5 - Hydration, Setting and Hardening of Portland Cement," in *Lea's Chemistry of Cement and Concrete (Fifth Edition)*, P. C. Hewlett and M. Liska, Eds., Butterworth-Heinemann, 2019, pp. 157–250. doi: 10.1016/B978-0-08-100773-0.00005-8.

[8] P. Mounanga, A. Khelidj, A. Loukili, and V. Baroghel-Bouny, "Predicting Ca (OH) $_2$ content and chemical shrinkage of hydrating cement pastes using analytical approach," *Cem. Concr. Res.*, vol. 34, no. 2, pp. 255–265, 2004.

[9] L. Lavagna and R. Nisticò, "An insight into the chemistry of cement—a review," *Appl. Sci.*, vol. 13, no. 1, p. 203, 2022.

[10] Y. Reches, "Nanoparticles as concrete additives: Review and perspectives," *Constr. Build. Mater.*, vol. 175, pp. 483–495, 2018.

[11] F. Sanchez and K. Sobolev, "Nanotechnology in concrete–a review," *Constr. Build. Mater.*, vol. 24, no. 11, pp. 2060–2071, 2010.

[12] J. Alonso, J. M. Barandiarán, L. F. Barquín, and A. García-Arribas, "Magnetic nanoparticles, synthesis, properties, and applications," in *Magnetic nanostructured materials*, Elsevier, 2018, pp. 1–40. Accessed: May 31, 2024.

[13] E. Harvey and M. Ghantasala, "Nanofabrication," in *Nanostructure control of materials*, Elsevier, 2006, pp. 303–330.

[14] M. C. Gonçalves and F. Margarido, Eds., *Materials for Construction and Civil Engineering: Science, Processing, and Design*. Cham: Springer International Publishing, 2015.

[15] M. M. Norhasri, M. S. Hamidah, and A. M. Fadzil, "Applications of using nano material in concrete: A review," *Constr. Build. Mater.*, vol. 133, pp. 91–97, 2017.

[16] T. A. Saleh, "Nanomaterials: Classification, properties, and environmental toxicities," *Environ. Technol. Innov.*, vol. 20, p. 101067, Nov. 2020,

[17] V. Singh, P. Yadav, and V. Mishra, "Recent Advances on Classification, Properties, Synthesis, and Characterization of Nanomaterials," in *Green Synthesis of Nanomaterials for Bioenergy Applications*, 1st ed., N. Srivastava, M. Srivastava, P. K. Mishra, and V. K. Gupta, Eds., Wiley, 2020, pp. 83–97.

[18] B. Mekuye and B. Abera, "Nanomaterials: An overview of synthesis, classification, characterization, and applications," *Nano Sel.*, vol. 4, no. 8, pp. 486–501, 2023.
[19] D.-Y. Yoo, T. Oh, and N. Banthia, "Nanomaterials in ultra-high-performance concrete (UHPC)–A review," *Cem. Concr. Compos.*, vol. 134, p. 104730, 2022.
[20] P. Aggarwal, R. P. Singh, and Y. Aggarwal, "Use of nano-silica in cement based materials—A review," *Cogent Eng.*, vol. 2, no. 1, p. 1078018, Dec. 2015.
[21] S. I. Ghazanlou, M. Jalaly, S. Sadeghzadeh, and A. H. Korayem, "A comparative study on the mechanical, physical and morphological properties of cement-micro/nanoFe3O4 composite," *Sci. Rep.*, vol. 10, no. 1, p. 2859, 2020.
[22] M. Cao, X. Ming, K. He, L. Li, and S. Shen, "Effect of macro-, micro-and nano-calcium carbonate on properties of cementitious composites—A review," *Materials*, vol. 12, no. 5, p. 781, 2019.
[23] A. G. Mehairi, R. Khoshnazar, and M. M. Husein, "Foamed concrete produced from CO2/N2 foam stabilized by CaCO3 nanoparticles and CTAB," *Constr. Build. Mater.*, vol. 424, p. 135927, 2024.
[24] P. Jaishankar and C. Karthikeyan, "Characteristics of cement concrete with nano alumina particles," in *IOP conference series: earth and environmental science*, IOP Publishing, 2017, p. 012005. Accessed: Apr. 24, 2024.
[25] Q. Liu, Q. Jiang, M. Huang, J. Xin, and P. Chen, "The fresh and hardened properties of 3D printing cement-base materials with self-cleaning nano-TiO2: An exploratory study," *J. Clean. Prod.*, vol. 379, p. 134804, 2022.
[26] A. Teymouri, A. H. Hossein, R. Khoshnazar, and H. J. Guzmán, "A review on carbon nanofiber production and application in cementitious mixtures," *J. Build. Eng.*, p. 108519, 2024.
[27] L. Yu and R. Wu, "Using graphene oxide to improve the properties of ultra-high-performance concrete with fine recycled aggregate," *Constr. Build. Mater.*, vol. 259, p. 120657, 2020.
[28] A. M. Onaizi, G. F. Huseien, N. H. A. S. Lim, M. Amran, and M. Samadi, "Effect of nanomaterials inclusion on sustainability of cement-based concretes: A comprehensive review," *Constr. Build. Mater.*, vol. 306, p. 124850, Nov. 2021.
[29] I. A. Rahman and V. Padavettan, "Synthesis of Silica Nanoparticles by Sol-Gel: Size-Dependent Properties, Surface Modification, and Applications in Silica-Polymer Nanocomposites—A Review," *J. Nanomater.*, vol. 2012, pp. 1–15, 2012.
[30] I. A. Rahman *et al.*, "An optimized sol–gel synthesis of stable primary equivalent silica particles," *Colloids Surf. Physicochem. Eng. Asp.*, vol. 294, no. 1–3, pp. 102–110, 2007.
[31] T. T. Y. Tan, S. Liu, Y. Zhang, M. Y. Han, and S. T. Selvan, "Microemulsion preparative methods (overview)," *Compr. Nanosci. Technol.*, pp. 399–441, 2011.
[32] G. A. Silva, "Introduction to nanotechnology and its applications to medicine," *Surg. Neurol.*, vol. 61, no. 3, pp. 216–220, 2004.
[33] E. F. Vansant, P. Van Der Voort, and K. C. Vrancken, *Characterization and chemical modification of the silica surface*. Elsevier, 1995. Accessed: Aug. 04, 2024.
[34] K. J. Klabunde and R. M. Richards, *Nanoscale materials in chemistry*. John Wiley & Sons, 2009. Accessed: Aug. 04, 2024.
[35] L. L. Hench and J. K. West, "The sol-gel process," *Chem. Rev.*, vol. 90, no. 1, pp. 33–72, Jan. 1990.
[36] W. Stöber, A. Fink, and E. Bohn, "Controlled growth of monodisperse silica spheres in the micron size range," *J. Colloid Interface Sci.*, vol. 26, no. 1, pp. 62–69, 1968.

[37] M. Alhawat, A. Ashour, and A. El-Khoja, “Properties of concrete incorporating different nano silica particles,” *Mater. Res. Innov.*, vol. 24, no. 3, pp. 133–144, Apr. 2020.
[38] E. Ghafari, H. Costa, E. Júlio, A. Portugal, and L. Durães, “The effect of nanosilica addition on flowability, strength and transport properties of ultra high performance concrete,” *Mater. Des.*, vol. 59, pp. 1–9, 2014.
[39] Q. Huang, X. Zhu, D. Liu, L. Zhao, and M. Zhao, “Modification of water absorption and pore structure of high-volume fly ash cement pastes by incorporating nanosilica,” *J. Build. Eng.*, vol. 33, p. 101638, 2021.
[40] P. Hou, X. Cheng, J. Qian, R. Zhang, W. Cao, and S. P. Shah, “Characteristics of surface-treatment of nano-SiO2 on the transport properties of hardened cement pastes with different water-to-cement ratios,” *Cem. Concr. Compos.*, vol. 55, pp. 26–33, 2015.
[41] M. Jalal, A. R. Pouladkhan, H. Norouzi, and G. Choubdar, “Chloride penetration, water absorption and electrical resistivity of high performance concrete containing nano silica and silica fume,” *J. Am. Sci.*, vol. 8, no. 4, pp. 278–284, 2012.
[42] K. Behfarnia and M. Rostami, “Effects of micro and nanoparticles of SiO2 on the permeability of alkali activated slag concrete,” *Constr. Build. Mater.*, vol. 131, pp. 205–213, 2017.
[43] M. Rupasinghe, R. San Nicolas, P. Mendis, M. Sofi, and T. Ngo, “Investigation of strength and hydration characteristics in nano-silica incorporated cement paste,” *Cem. Concr. Compos.*, vol. 80, pp. 17–30, 2017.
[44] F. Torabian Isfahani, E. Redaelli, F. Lollini, W. Li, and L. Bertolini, “Effects of nanosilica on compressive strength and durability properties of concrete with different water to binder ratios,” *Adv. Mater. Sci. Eng.*, vol. 2016, 2016.
[45] A. AlKhatib, M. Maslehuddin, and S. U. Al-Dulaijan, “Development of high performance concrete using industrial waste materials and nano-silica,” *J. Mater. Res. Technol.*, vol. 9, no. 3, pp. 6696–6711, 2020.
[46] A. N. Givi, S. A. Rashid, F. N. A. Aziz, and M. A. M. Salleh, “Experimental investigation of the size effects of SiO2 nano-particles on the mechanical properties of binary blended concrete,” *Compos. Part B Eng.*, vol. 41, no. 8, pp. 673–677, 2010.
[47] H. Madani, A. Bagheri, and T. Parhizkar, “The pozzolanic reactivity of monodispersed nanosilica hydrosols and their influence on the hydration characteristics of Portland cement,” *Cem. Concr. Res.*, vol. 42, no. 12, pp. 1563–1570, 2012.
[48] S. Bai, X. Guan, H. Li, and J. Ou, “Effect of the specific surface area of nano-silica particle on the properties of cement paste,” *Powder Technol.*, vol. 392, pp. 680–689, Nov. 2021.
[49] M. Tabish, M. M. Zaheer, and A. Baqi, “Effect of nano-silica on mechanical, microstructural and durability properties of cement-based materials: A review,” *J. Build. Eng.*, vol. 65, p. 105676, 2023.
[50] X. Zhang, H. Yang, Q. Yang, X. Du, C. Li, and X. Cheng, “Effects of particle size of colloidal nanosilica on hydration of Portland cement at early age,” *Adv. Mech. Eng.*, vol. 11, no. 2, p. 168781401982894, Feb. 2019.
[51] S. Li, W. Chao, W. Li, J. Cheng, and B. Yuan, “Study on the effect of nanosilica suspension on the properties of cement-based grouts,” *Mater. Sci.-Pol.*, vol. 40, no. 4, pp. 171–182, Dec. 2022.
[52] A. Mohammed *et al.*, “Microstructure characterizations, thermal properties, yield stress, plastic viscosity and compression strength of cement paste modified with nanosilica,” *J. Mater. Res. Technol.*, vol. 9, no. 5, pp. 10941–10956, 2020.

[53] M. Bolhassani and M. Samani, “Effect of type, size, and dosage of nanosilica and microsilica on properties of cement paste and mortar,” *ACI Mater. J.*, vol. 112, no. 2, pp. 1–7, 2015.
[54] S. Haruehansapong, T. Pulngern, and S. Chucheepsakul, “Effect of the particle size of nanosilica on the compressive strength and the optimum replacement content of cement mortar containing nano-SiO2,” *Constr. Build. Mater.*, vol. 50, pp. 471–477, Jan. 2014, doi: 10.1016/j.conbuildmat.2013.10.002.
[55] A. Khaloo, M. H. Mobini, and P. Hosseini, “Influence of different types of nano-SiO2 particles on properties of high-performance concrete,” *Constr. Build. Mater.*, vol. 113, pp. 188–201, 2016.
[56] M. T. Maagi and G. Jun, “Effect of the particle size of nanosilica on early age compressive strength in oil-well cement paste,” *Constr. Build. Mater.*, vol. 262, p. 120393, Nov. 2020.
[57] T. Meng, Y. Hong, H. Wei, and Q. Xu, “Effect of nano-SiO2 with different particle size on the hydration kinetics of cement,” *Thermochim. Acta*, vol. 675, pp. 127–133, 2019.
[58] S. Haruehansapong, T. Pulngern, and S. Chucheepsakul, “Effect of Nanosilica Particle Size on the Water Permeability, Abrasion Resistance, Drying Shrinkage, and Repair Work Properties of Cement Mortar Containing Nano-SiO_2,” *Adv. Mater. Sci. Eng.*, vol. 2017, p. e4213690, Apr. 2017.
[59] M. Kooshafar and H. Madani, “An investigation on the influence of nano silica morphology on the characteristics of cement composites,” *J. Build. Eng.*, vol. 30, p. 101293, Jul. 2020.
[60] H. Xiao, F. Zhang, R. Liu, R. Zhang, Z. Liu, and H. Liu, “Effects of pozzolanic and non-pozzolanic nanomaterials on cement-based materials,” *Constr. Build. Mater.*, vol. 213, pp. 1–9, 2019.
[61] H. Sun, X. Zhang, P. Zhao, and D. Liu, “Effects of Nano-Silica Particle Size on Fresh State Properties of Cement Paste,” *KSCE J. Civ. Eng.*, vol. 25, no. 7, pp. 2555–2566, Jul. 2021.
[62] T. Meng, K. Ying, Y. Hong, and Q. Xu, “Effect of different particle sizes of nano-SiO_2 on the properties and microstructure of cement paste,” *Nanotechnol. Rev.*, vol. 9, no. 1, pp. 833–842, Sep. 2020.
[63] J. D. Puerto Suárez, G. N. Hernández Guarin, and J. Lizarazo-Marriaga, “Effect of nanosilica particles on the rheological and mechanical properties of cement pastes using polyhydroxyl and polycarboxylate-based superplasticizers,” *Eur. J. Environ. Civ. Eng.*, vol. 24, no. 13, pp. 2230–2254, Nov. 2020.
[64] K. Khan, M. A. M. Johari, M. N. Amin, and M. Iqbal, “Evaluation of the mechanical properties, microstructure, and environmental impact of mortar incorporating metakaolin, micro and nano-silica,” *Case Stud. Constr. Mater.*, vol. 20, p. e02699, 2024.
[65] R. S. Fernandes, I. M. Raimundo Jr, and M. F. Pimentel, “Revising the synthesis of Stöber silica nanoparticles: A multivariate assessment study on the effects of reaction parameters on the particle size,” *Colloids Surf. Physicochem. Eng. Asp.*, vol. 577, pp. 1–7, 2019.
[66] W. Gao, M. Rigout, and H. Owens, “Facile control of silica nanoparticles using a novel solvent varying method for the fabrication of artificial opal photonic crystals,” *J. Nanoparticle Res.*, vol. 18, no. 12, p. 387, Dec. 2016.
[67] K. Lee, A. N. Sathyagal, and A. V. McCormick, “A closer look at an aggregation model of the Stöber process,” *Colloids Surf. Physicochem. Eng. Asp.*, vol. 144, no. 1–3, pp. 115–125, 1998.
[68] “Standard Practice for Mechanical Mixing of Hydraulic Cement Pastes and Mortars of Plastic Consistency.” Accessed: Feb. 18, 2024. [Online]. Available: https://www.astm.org/c0305-20.html

[69] “Standard Test Method for Measurement of Heat of Hydration of Hydraulic Cementitious Materials Using Isothermal Conduction Calorimetry.” Accessed: Feb. 18, 2024. [Online]. Available: https://www.astm.org/c1702-17.html
[70] K. Scrivener, R. Snellings, and B. Lothenbach, *A practical guide to microstructural analysis of cementitious materials*. Crc Press, 2018. Accessed: Dec. 14, 2023. [Online].
[71] N. Doebelin and R. Kleeberg, “Profex: a graphical user interface for the Rietveld refinement program BGMN,” *J. Appl. Crystallogr.*, vol. 48, no. 5, pp. 1573–1580, 2015.
[72] E. John and B. Lothenbach, “Cement hydration mechanisms through time – a review,” *J. Mater. Sci.*, vol. 58, no. 24, pp. 9805–9833, Jun. 2023.
[73] P. F. G. Banfill and D. C. Saunders, “On the viscometric examination of cement pastes,” *Cem. Concr. Res.*, vol. 11, no. 3, pp. 363–370, 1981.
[74] D. Feys, J. E. Wallevik, A. Yahia, K. H. Khayat, and O. H. Wallevik, “Extension of the Reiner–Riwlin equation to determine modified Bingham parameters measured in coaxial cylinders rheometers,” *Mater. Struct.*, vol. 46, no. 1–2, pp. 289–311, Jan. 2013.
[75] Q. Yuan, C. Shi, and D. Jiao, *Rheology of Fresh Cement-Based Materials: Fundamentals, Measurements, and Applications*. CRC Press, 2022. Accessed: Dec. 18, 2023. [Online].
[76] J. Sun, Z. Xu, W. Li, and X. Shen, “Effect of nano-SiO2 on the early hydration of alite-sulphoaluminate cement,” *Nanomaterials*, vol. 7, no. 5, p. 102, 2017.
[77] R. J. A. Sldozian, “Comparison between the properties of Amorphous and Crystalline-Nano SiO2 additives on Concrete,” *Int. J. Sci. Eng. Res.*, vol. 5, no. 6, pp. 592–598, 2014.
[78] S. H. Araghi, M. H. Entezari, and M. Chamsaz, “Modification of mesoporous silica magnetite nanoparticles by 3-aminopropyltriethoxysilane for the removal of Cr (VI) from aqueous solution,” *Microporous Mesoporous Mater.*, vol. 218, pp. 101–111, 2015.
[79] S. S. Shafqat *et al.*, “Development of amino-functionalized silica nanoparticles for efficient and rapid removal of COD from pre-treated palm oil effluent,” *J. Mater. Res. Technol.*, vol. 8, no. 1, pp. 385–395, 2019.
[80] S. Soontaranon, W. Limphirat, and S. Pratapa, “XRD, WAXS, FTIR, and XANES studies of silica-zirconia systems,” *Ceram. Int.*, vol. 45, no. 12, pp. 15660–15670, 2019.
[81] M. Marrone *et al.*, “A Fourier Transform Infrared (FTIR) Study of the Reaction of Triethoxysilane (TES) and Bis[3-triethoxysilylpropyl]tetrasulfane (TESPT) with the Surface of Amorphous Silica,” *J. Phys. Chem. B*, vol. 108, no. 11, pp. 3563–3572, Mar. 2004.
[82] P. Vejayakumaran, I. A. Rahman, C. S. Sipaut, J. Ismail, and C. K. Chee, “Structural and thermal characterizations of silica nanoparticles grafted with pendant maleimide and epoxide groups,” *J. Colloid Interface Sci.*, vol. 328, no. 1, pp. 81–91, 2008.
[83] L. Zhou, W. Yuan, J. Yuan, and X. Hong, “Preparation of double-responsive SiO2-g-PDMAEMA nanoparticles via ATRP,” *Mater. Lett.*, vol. 62, no. 8–9, pp. 1372–1375, 2008.
[84] W.-W. Kim and J.-H. Moon, “Analysis of Mechanical Properties and Microstructure of Nano- and Micro-SiO2 Materials as Cementitious Composite Binder,” *Int. J. Concr. Struct. Mater.*, vol. 17, no. 1, p. 68, Nov. 2023.
[85] H. Chen, P. Feng, Y. Du, J. Jiang, and W. Sun, “The effect of superhydrophobic nano-silica particles on the transport and mechanical properties of hardened cement pastes,” *Constr. Build. Mater.*, vol. 182, pp. 620–628, 2018.
[86] P. Hou, S. Kawashima, D. Kong, D. J. Corr, J. Qian, and S. P. Shah, “Modification effects of colloidal nanoSiO2 on cement hydration and its gel property,” *Compos. Part B Eng.*, vol. 45, no. 1, pp. 440–448, 2013.

[87] S. Ghasemalizadeh and R. Khoshnazar, “Compressive Strength and Microstructural Development of Cementitious Mixtures Incorporating Ultrafine Granulated Blast Furnace Slag,” *J. Mater. Civ. Eng.*, vol. 36, no. 2, p. 04023572, Feb. 2024.
[88] V. Jafari, A. Allahverdi, and M. Vafaei, “Ultrasound-assisted synthesis of colloidal nanosilica from silica fume: Effect of sonication time on the properties of product,” *Adv. Powder Technol.*, vol. 25, no. 5, pp. 1571–1577, Sep. 2014.
[89] Y. El Bitouri, “Rheological Behavior of Cement Paste: A Phenomenological State of the Art,” *Eng*, vol. 4, no. 3, Art. no. 3, Sep. 2023.
[90] Y. Peng, K. Ma, G. Long, and Y. Xie, “Influence of nano-SiO_2, nano-$CaCO_3$ and nano-Al_2O_3 on rheological properties of cement–fly ash paste,” *Materials*, vol. 12, no. 16, p. 2598, 2019.
[91] F.-J. Rubio-Hernández, “Rheological Behavior of Fresh Cement Pastes,” *Fluids*, vol. 3, no. 4, Art. no. 4, Dec. 2018.
[92] Y. C. Flores, G. C. Cordeiro, R. D. Toledo Filho, and L. M. Tavares, “Performance of Portland cement pastes containing nano-silica and different types of silica,” *Constr. Build. Mater.*, vol. 146, pp. 524–530, 2017.
[93] F. Lavergne, R. Belhadi, J. Carriat, and A. Ben Fraj, “Effect of nano-silica particles on the hydration, the rheology and the strength development of a blended cement paste,” *Cem. Concr. Compos.*, vol. 95, pp. 42–55, Jan. 2019.
[94] A. Leemann and F. Winnefeld, “The effect of viscosity modifying agents on mortar and concrete,” *Cem. Concr. Compos.*, vol. 29, no. 5, pp. 341–349, May 2007.
[95] G. H. Bogush, M. A. Tracy, and C. F. Zukoski Iv, “Preparation of monodisperse silica particles: control of size and mass fraction,” *J. Non-Cryst. Solids*, vol. 104, no. 1, pp. 95–106, 1988.

Appendix A

Effect of Synthesis Parameters on the Particle Size and Zeta Potential of Nanosilica Particles

In the Section 3.2.1 of this thesis, the effect of different amounts of ethanol on the particle size and zeta potential of the nanosilica particles was reported. To investigate the effect of other synthesis parameters including the amount of ammonia and aging time, additional experiments were conducted, and the results are presented in **Table A**.

A set of experiments were defined to investigate the effect of ammonia content, that was important for the control of pH, on the particle size of nanosilica samples. Ethanol with the amount of 40 mL was mixed with 80 mL of distilled water. Then, ammonia with the amount of 7.5, 10 or 20 mL was added to this solution. This was followed by adding 12.5 mL of TEOS. The increase in the ammonia content increases the hydrolysis and condensation rate, therefore increasing the nanosilica particle size [30], [95]. All the other steps were the same as previous experiment sets which was mentioned in Section 3.2.1.

The effect of aging time on the nanosilica particle size was also investigated. This term referred to the period during which magnetic stirring would last. This effect was explored through synthesis of the nanosilica samples with 15 mL ammonia, 40 mL ethanol and aging time of 60 h. As a result, the nanosilica particle size increased with this procedure and exceeded 100 nm. This might be attributed to the dissolution of fine particles and their reprecipitation on the surface of larger particles, leading to their growth. The hydrodynamic diameter and ζ-Potential of each nanosilica sample were measured and presented in **Table A**.

Table A: Synthesis parameters of nanosilica, hydrodynamic diameter (D_h), and ζ-Potential.

	Sample ID	Variables					Characteristics	
		TEOS (mL)	Water (mL)	Ammonia (mL)	Ethanol (mL)	Aging (h)	D_h (nm)	ζ-Potential (mV)
Effect of Ammonia content	N6	12.5	80	7.5	40	20	43	-45
	N7			10			51	-43
	N8			20			93	-31
Effect of Aging	N9	12.5	80	15	40	60	126	-39

Appendix B

Size Distribution of Nanosilica Particles based on TEM Images

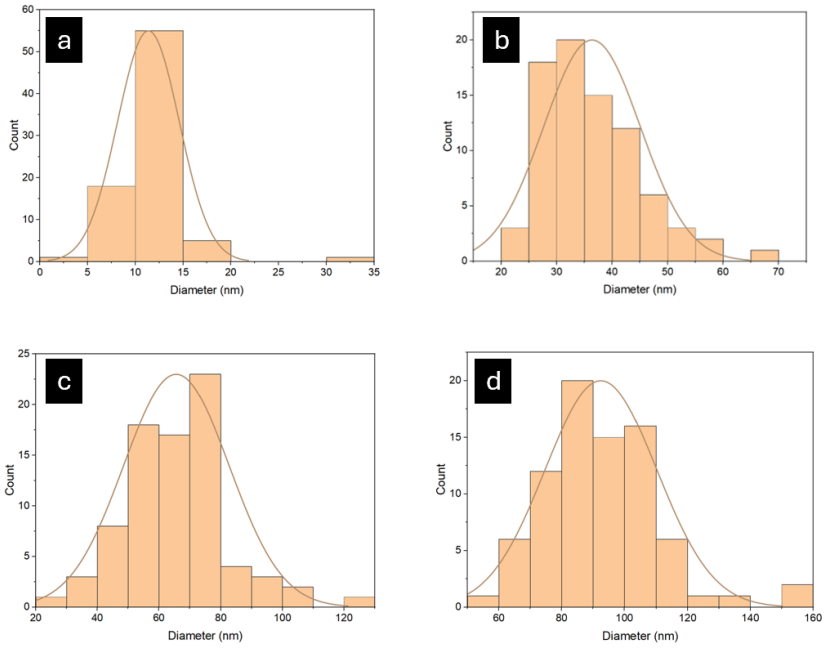

Figure B: Nanosilica particle size distribution based on TEM image analysis, a) NS10, b) NS35, c) NS65, and d) NS90.

Appendix C

Method for the Calculation of Hydration Acceleration Period in Cement Paste based on Heat Flow Curve

To calculate the hydration acceleration period in cement paste, three important times of T1, T2 and T3 were extracted from the heat flow curve. In this context, T1 refers to the time when the exothermic rate of hydration reaches its minimum. T2 is the time corresponding to the intersection point between the linear portion of the acceleration period and a line parallel to the T1 time axis, while T3 represents the time at which the exothermic rate reaches its peak. These three critical points are used to calculate the duration of the acceleration period (T3 - T2) [48]. These points are shown in **Figure C**.

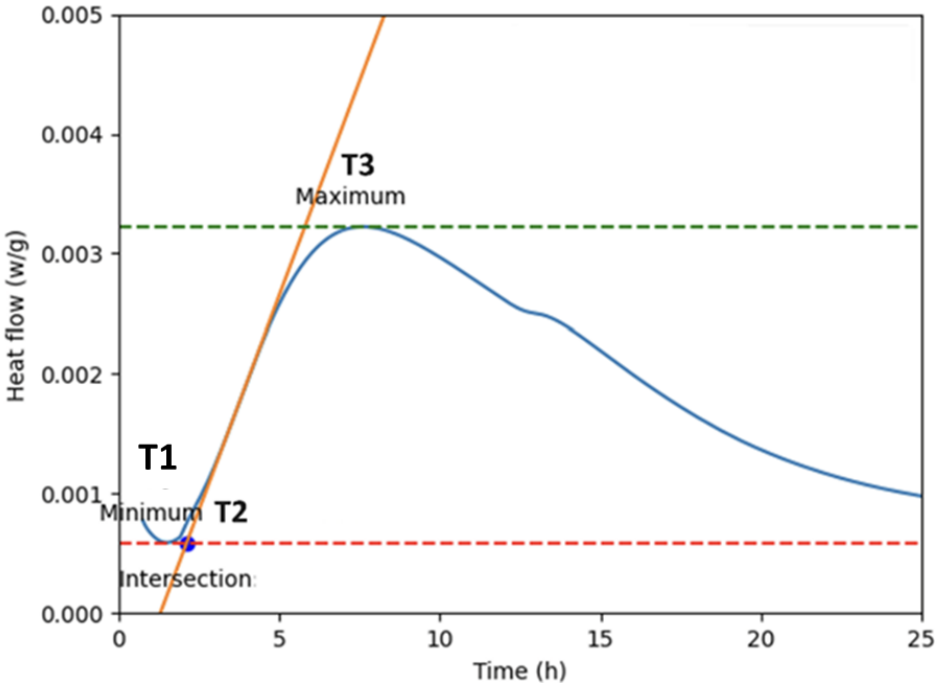

Figure C: Calculation of hydration acceleration period in a Portland cement paste.

Appendix D

XRD Patterns of Cement Pastes with 2 wt% Nanosilica Compared to the Reference Paste

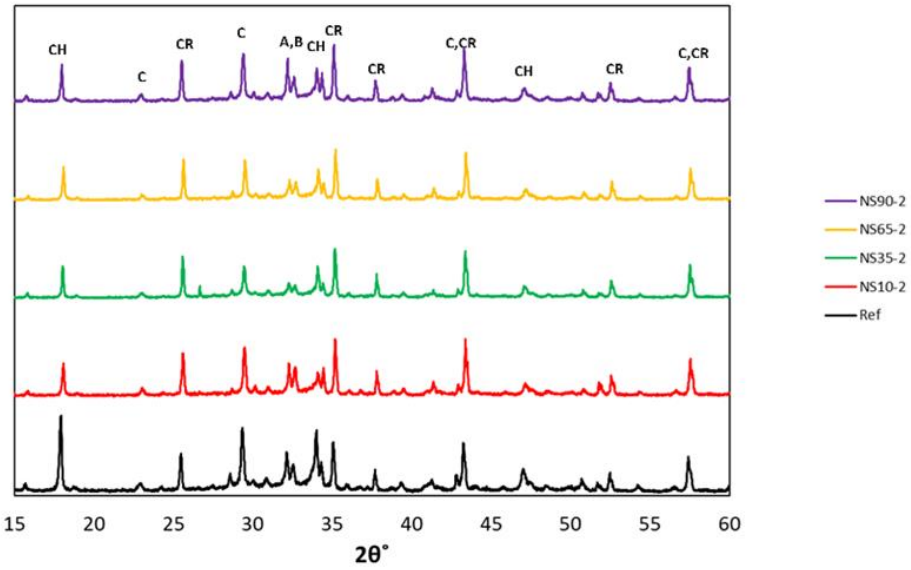

Figure D1: XRD patterns for cement paste with 2 wt% nanosilica of different sizes at 1 day compared to the reference paste [Calcium hydroxide (CH), Calcite (C), Corundum (CR), C_3S (A), C_2S (B)].

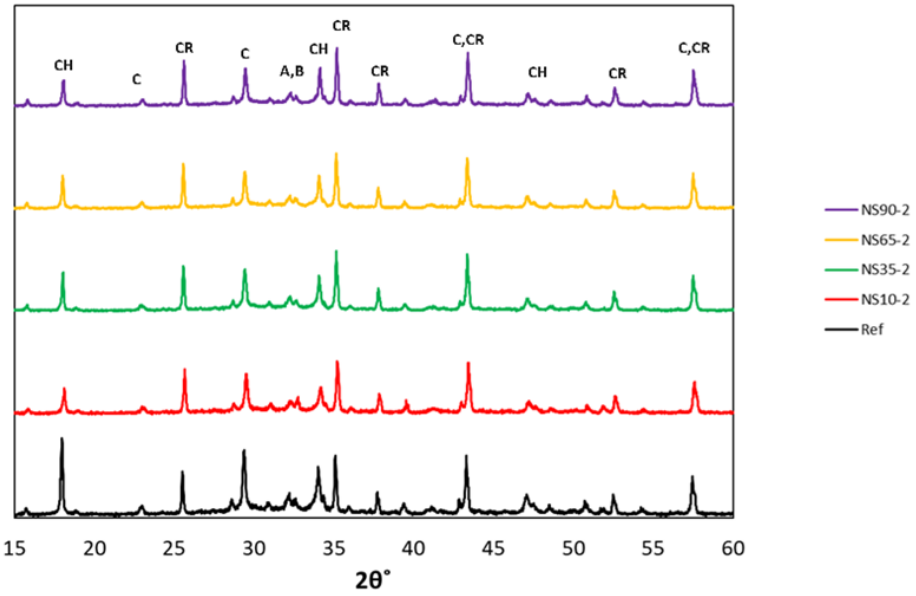

Figure D2: XRD patterns for cement paste with 2 wt% nanosilica of different sizes at 7 days compared to the reference paste [Calcium hydroxide (CH), Calcite (C), Corundum (CR), C_3S (A), C_2S (B)].

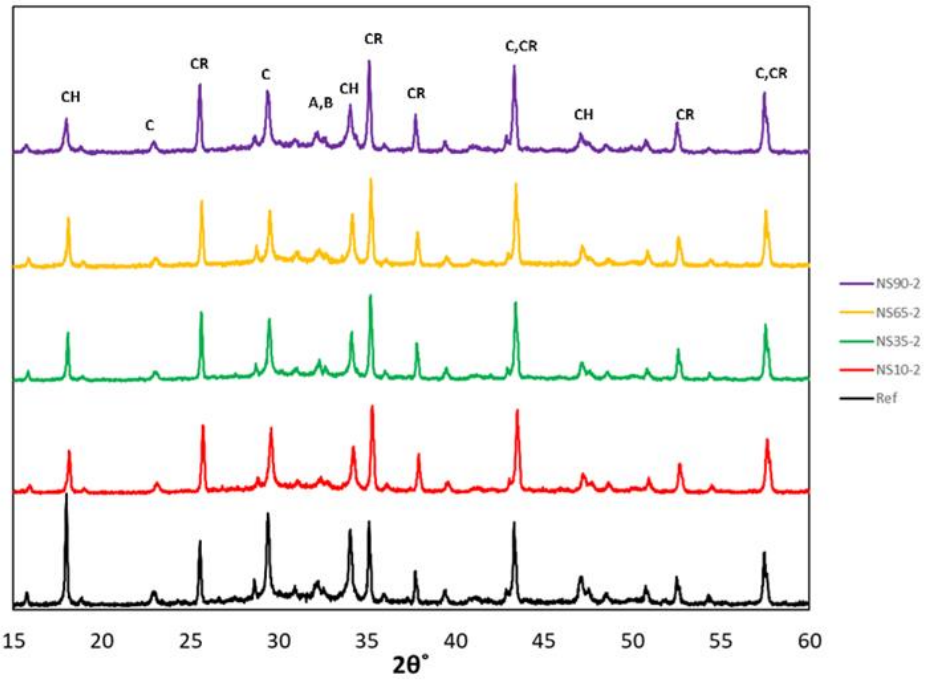

Figure D3: XRD patterns for cement paste with 2 wt% nanosilica of different sizes at 28 days compared to the reference paste [Calcium hydroxide (CH), Calcite (C), Corundum (CR), C_3S (A), C_2S (B)].

Appendix E

Viscosity and Yield Stress of Cement Pastes as determined by the Modified Bingham Model

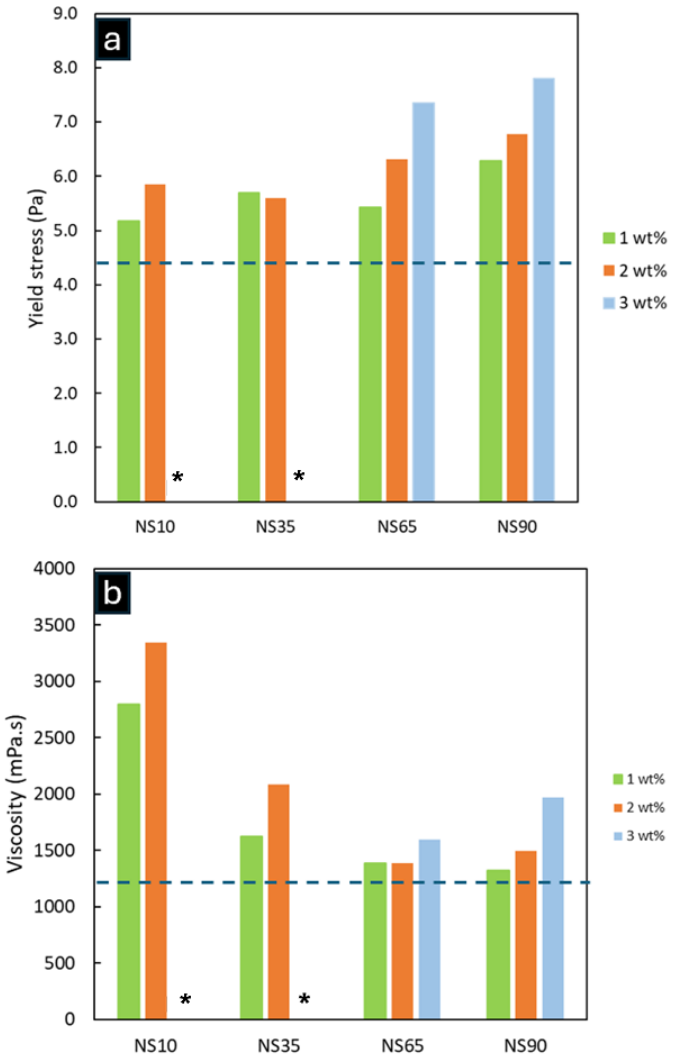

Figure E: a) Yield stress, and b) Viscosity of cement paste with 1, 2 and 3 wt% nanosilica based on MB model. Dashed lines represent results for the reference paste.

*Data for NS10, NS35 at 3 wt% are not available due to very high viscosity of the paste.

Appendix F

SEM image of the reference cement paste and cement paste with 2wt % NS10 at the age of 150 days

Figure F shows that the addition of 2 wt% NS10 has resulted in a denser microstructure compared to the reference paste. Such densification of the cement paste microstructure contributes to improved engineering properties, such as higher compressive strength of the paste.

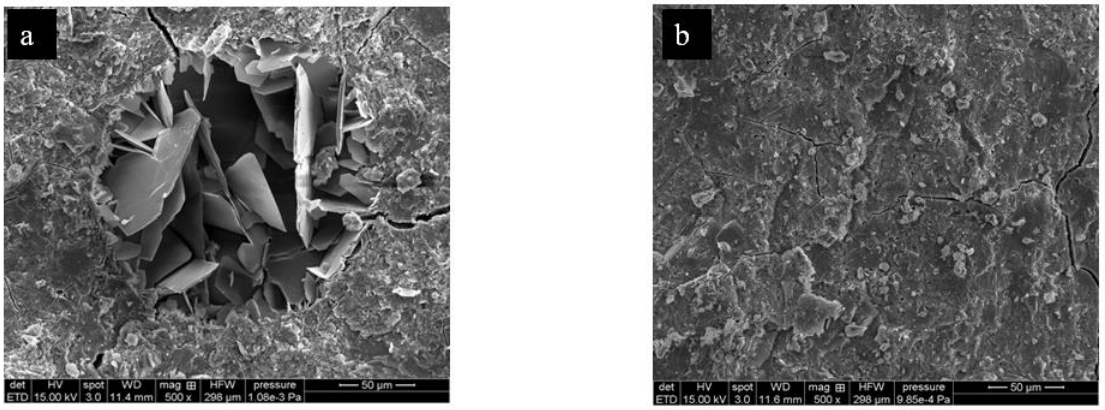

Figure F: SEM image of a) reference cement paste b) cement paste with 2 wt% NS10.

Appendix G

Copyright permission materials